Eur. Phys. J. Special Topics **229**, 3085–3141 (2020)

https://doi.org/10.1140/epjst/e2020-000020-x

THE EUROPEAN PHYSICAL JOURNAL SPECIAL TOPICS

Review

Status of weak scale supersymmetry after LHC Run 2 and ton-scale noble liquid WIMP searches

Howard Baer[1,a], Vernon Barger[2], Dibyashree Sengupta[1], Shadman Salam[1], and Kuver Sinha[1]

[1] Department of Physics and Astronomy, University of Oklahoma, Norman, OK 73019, USA
[2] Department of Physics, University of Wisconsin, Madison, WI, 53706, USA

Received 10 February 2020 / Accepted 30 September 2020
Published online 14 December 2020

Abstract. After completion of LHC Run 2, the ATLAS and CMS experiments had collected of order 139 fb^{-1} of data at $\sqrt{s} = 13$ TeV. While discovering a very Standard Model-like Higgs boson of mass $m_h \simeq 125$ GeV, no solid signal for physics beyond the Standard Model has emerged so far at LHC. In addition, no WIMP signals have emerged so far at ton-scale noble liquid WIMP search experiments. For the case of weak scale supersymmetry (SUSY), which is touted as a simple and elegant solution to the gauge hierarchy problem and likely low energy limit of compactified string theory, LHC has found rather generally that gluinos are beyond about 2.2 TeV whilst top squark must lie beyond 1.1 TeV. These limits contradict older simplistic notions of naturalness that emerged in the 1980s–1990s, leading to the rather pessimistic view that SUSY is now excluded except for perhaps some remaining narrow corners of parameter space. Yet, this picture ignores several important developments in SUSY/string theory that emerged in the 21st century: 1. the emergence of the string theory landscape and its solution to the cosmological constant problem, 2. a more nuanced view of naturalness including the notion of "stringy naturalness", 3. the emergence of anomaly-free discrete R-symmetries and their connection to R-parity, Peccei-Quinn symmetry, the SUSY μ problem and proton decay and 4. the importance of including a solution to the strong CP problem. Rather general considerations from the string theory landscape favor large values of soft terms, subject to the vacuum selection criteria that electroweak symmetry is properly broken (no charge and/or color breaking (CCB) minima) and the resulting magnitude of the weak scale is not too far from our measured value. Then stringy naturalness predicts a Higgs mass $m_h \sim 125$ GeV whilst sparticle masses are typically lifted beyond present LHC bounds. In light of these refinements in theory perspective confronted by LHC and dark matter search results, we review the most likely LHC, ILC and dark matter signatures that are expected to arise from weak scale SUSY as we understand it today.

[a] e-mail: baer@nhn.ou.edu

1 Introduction

1.1 Why SUSY?

The discovery in 2012 of the Higgs boson with mass $m_h \simeq 125$ GeV by the ATLAS [1] and CMS [2] collaborations at LHC seemingly completes the Standard Model (SM), and yet brings with it a puzzle. It was emphasized as early as 1978 by Wilson and Susskind [3] that fundamental scalar particles are unnatural in quantum field theory. In the case of the SM Higgs boson with a doublet of Higgs scalars ϕ and Higgs potential given by

$$V = -\mu^2 \phi^\dagger \phi + \lambda (\phi^\dagger \phi)^2, \tag{1}$$

one expects a physical Higgs boson mass value

$$m_h^2 \simeq 2\mu^2 + \delta m_h^2, \tag{2}$$

where the leading radiative correction is given by

$$\delta m_h^2 \simeq \frac{3}{4\pi^2}\left(-\lambda_t^2 + \frac{g^2}{4} + \frac{g^2}{8\cos^2\theta_W} + \lambda\right)\Lambda^2. \tag{3}$$

In the above expression, λ_t is the top quark Yukawa coupling, g is the $SU(2)$ gauge coupling and λ is the Higgs field quartic coupling. The quantity Λ is the UV energy cutoff to otherwise divergent loop integrals. Taking Λ as high as the reduced Planck mass $m_P \simeq 2.4 \times 10^{18}$ GeV would require a tuning of μ^2 to 30 decimal places to maintain the measured value of m_h^2. Alternatively, the notion of:

> **practical naturalness:** that *independent* contributions to any observable $\mathcal{O}$ be comparable to or less than $\mathcal{O}$,

then requires that loop integrals be truncated at $\Lambda \sim 1$ TeV. The situation is plotted in Figure 1: as Λ increases, then the free parameter μ^2 must be finely-tuned to large opposite-sign values so as to maintain m_h at its measured value. Such fine-tunings are regarded as symptomatic of some missing ingredient in the theory which, were it present, would render the theory natural.

In equation (3), various divergences appear involving the various fermion Yukawa couplings, the electroweak (EW) gauge couplings and the Higgs self-coupling λ. The unique solution which tames all these divergences at once is the inclusion of $N = 1$ supersymmetry (SUSY) into the theory [4,5]. SUSY extends the Poincare spacetime group of symmetries to its more general structure, the super-Poincare group, which includes anti-commutation relations as well as commutators. Under SUSY, fields are elevated to superfields which then express the Fermi-Bose symmetry inherent in the theory. Supersymmetrization of the SM to the well-behaved Minimal Supersymmetric Standard Model [6] (MSSM) requires an additional Higgs doublet to cancel triangle anomalies and to give mass to all the SM quarks and leptons under EW symmetry breaking. In the MSSM, then all quadratic divergences neatly cancel, leaving only log divergences. Since the log of a large number can be a small number, the Higgs mass instability is tamed and the weak scale can co-exist with higher mass scales: m_{PQ}, m_{GUT}, m_{string} etc. Inclusion of soft SUSY breaking terms can lift the predicted sparticles to the TeV scale in accord with constraints from collider searches. Under inclusion of R-parity conservation, the lightest SUSY particle (LSP) is stable and if it is electrically and color neutral, then it may be a good weakly interacting massive particle (WIMP) dark matter candidate. The MSSM with global, broken SUSY is

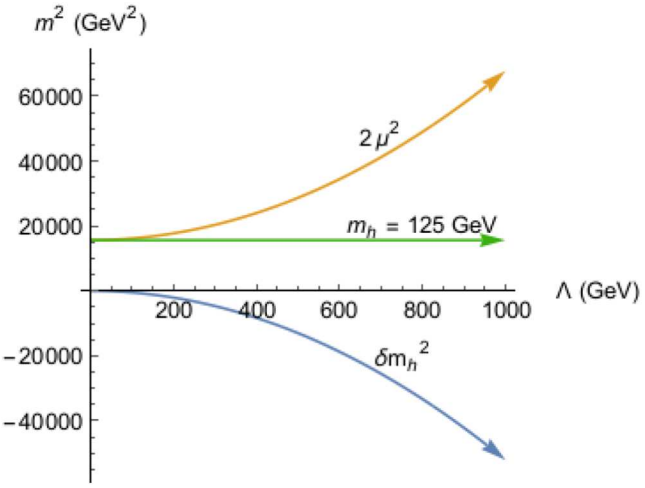

Fig. 1. Plot of measured Higgs mass squared along with radiative correction and tree-level term $2\mu^2$. For a given value of Λ, the μ^2 term must be adjusted (fine-tuned) to guarantee that $m_h = 125$ GeV.

expected to be the low energy effective theory of more encompassing local SUSY (supergravity) theories which in turn are the low energy effective theory expected from compactified string theory.

While SUSY elegantly solves the gauge hierarchy problem, it is actually supported by four sets of data via radiative corrections.

- The measured values of the three SM gauge couplings, when extrapolated to the grand unification scale $m_{GUT} \sim 2 \times 10^{16}$ GeV, meet at a point under renormalization group (RG) evolution [7–10]; this is not so in the SM or other beyond-the-SM (BSM) extensions.

- In the MSSM at the weak scale, EW symmetry is not expected to be broken using generic values for the soft SUSY breaking terms. Under RG evolution from some high scale (such as m_{GUT}), then the large value of the top Yukawa coupling drives the soft term $m_{H_u}^2$ to negative values causing EW symmetry to appropriately break [11–19]. This would not happen if the top mass $m_t \lesssim 100$ GeV.

- The value of the newly discovered Higgs boson $m_h \simeq 125$ GeV falls neatly within the narrow allowed window of MSSM values 115 GeV $< m_h \lesssim 135$ GeV, but only if radiative corrections from the top-squark sector are large enough [20,21]. Such a high value of m_h is consistent with highly mixed TeV-scale top squarks which are beyond current LHC reach. In the SM, no particular range of m_h is preferred other than that $m_h \lesssim 1$ TeV from unitarity constraints: see Figure 2.

- Precision EW calculation of m_W vs. m_t actually prefer the MSSM with heavy ($\gtrsim$1 TeV) SUSY particles over the SM [22].

It is hard to believe the consistency of all these radiative effects with the existence of weak scale SUSY (WSS) is just a coincidence. Historically, radiative corrections have been a reliable guide to new physics. It is important to remember that many new particles (W, Z bosons, top quark, Higgs boson etc.) have been reliably presaged by radiative corrections well before actual discovery: so may it be with SUSY.

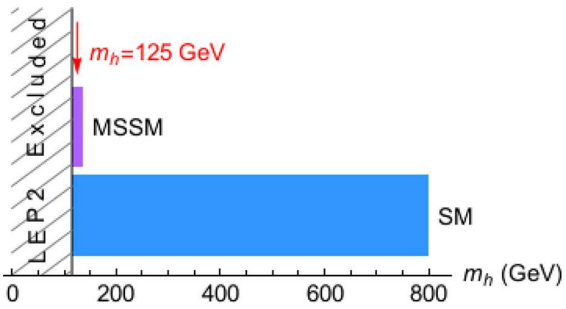

Fig. 2. Range of Higgs mass m_h predicted in the Standard Model compared to range of Higgs mass predicted by the MSSM. We also show the measured value of the Higgs mass by the arrow. The left-most region had been excluded by LEP2 searches prior to the LHC8 run.

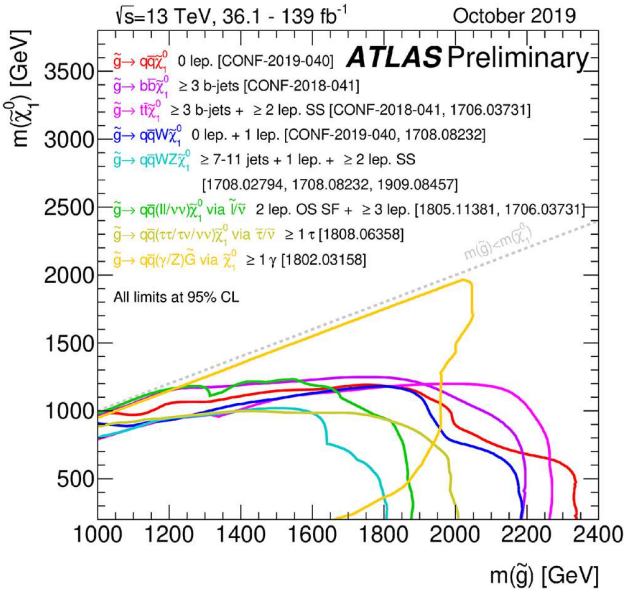

Fig. 3. Results of ATLAS searches for gluino pair production in SUSY for various simplified models with up to 139 fb^{-1} of data at $\sqrt{s} = 13$ TeV.

1.2 Where are the sparticles? LHC Run 2 SUSY search results

The question du jour is then: where are the predicted sparticles and where are the expected WIMPs? In Figure 3, we show recent 95% CL search limits for gluino pair production within various simplified models as deduced by the ATLAS experiment [23]. The data sets vary from 36–139 fb^{-1} at $\sqrt{s} = 13$ TeV. The plot is made in the $m_{\tilde{g}}$ vs. $m_{\widetilde{\chi}_1^0}$ mass plane. From the plot, we see that for relatively light values of $m_{\widetilde{\chi}_1^0} \lesssim 500$ GeV, then the approximate bound from LHC searches is that $m_{\tilde{g}} \gtrsim 2.2$ TeV. Limits from CMS are comparable [24].

In Figure 4, we show similar limits on searches for top-squark pair production in the $m_{\tilde{t}_1}$ vs. $m_{\widetilde{\chi}_1^0}$ plane for various simplified models with again 36–139 fb^{-1} of integrated luminosity at $\sqrt{s} = 13$ TeV. For $m_{\widetilde{\chi}_1^0} \lesssim 300$ GeV, then it is required that $m_{\tilde{t}_1} \gtrsim 1$ TeV [25,26].

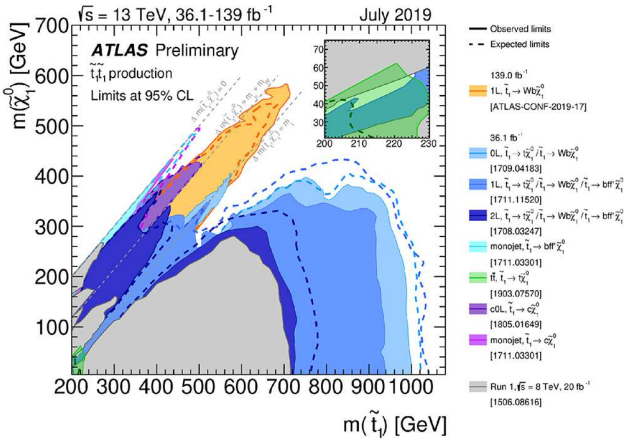

Fig. 4. Results of ATLAS searches for top squark pair production in SUSY for various simplified models with up to 139 fb^{-1} of data at $\sqrt{s} = 13$ TeV.

Many other searches for SUSY particles have been undertaken by ATLAS and CMS. A recent comprehensive review of LHC SUSY searches has been presented by Canepa [27]. Suffice it to say: so far, no compelling evidence for SUSY has emerged at LHC.

1.3 Where are the WIMPs?

Along with non-appearance of sparticles at LHC, we must also be concerned with the as-yet non-appearance of WIMPs at direct and/or indirect WIMP detection experiments. The current limits from the Xe-1ton experiment are shown in Figure 5 [28]. Here, the limits are placed in spin-independent (SI) WIMP-nucleon scattering cross section $\sigma^{SI}(\widetilde{\chi}_1^0 p)$ vs. $m_{\widetilde{\chi}_1^0}$ plane. Limits from Xe100, LUX (2017), PandaX (2017), Xe-1ton (2017) and Xe-1ton (1-ton-year exposure) are shown. At present, the latter limit is strongest and for a 100 GeV WIMP excludes $\sigma^{SI}(\widetilde{\chi}_1^0 p) \gtrsim 10^{-10}$ pb. For comparison, the popular hyperbolic branch/focus-point [29–31] (HB/FP) and many models with well-tempered neutralinos [32–34] predicted a direct detection cross section $\sigma^{SI}(\widetilde{\chi}_1^0 p) \sim 10^{-8}$ pb, relatively independent of $m_{\widetilde{\chi}_1^0} \sim 0.1{-}1$ TeV. Thus, these popular models are excluded by 1–2 orders of magnitude (depending on the value of $m_{\widetilde{\chi}_1^0}$).

1.4 Comparison to expectations from naturalness

The concept of naturalness can provide upper bounds on Higgs boson and sparticle masses. The results depend strongly on the definition of naturalness which is used. In Table 1, we list sparticle mass bounds derived from reference [35] using the $\Delta_{BG} \equiv max_i |\frac{\partial \ln m_Z^2}{\partial \ln p_i}|$ measure with $\Delta_{BG} < 10$, corresponding to $\Delta_{BG}^{-1} = 10\%$ fine-tuning. The p_i are taken as fundamental parameters of the theory, which in this case are the various soft terms and μ parameter from the mSUGRA/CMSSM [36–39] model. From Table 1, we see upper limits of $m_{\tilde{g}} \lesssim 400$ GeV while most other sparticles are not too far from the weak scale (defined as $m_{weak} \simeq m_{W,Z,h} \sim 100$ GeV). What is immediately of note is that current LHC gluino mass bounds are a factor five beyond the naturalness limits. Also, bounds on chargino masses from LEP2 ($m_{\widetilde{\chi}_1^\pm} > 103.5$ GeV) were already barely above the BG naturalness bounds. In the table, we

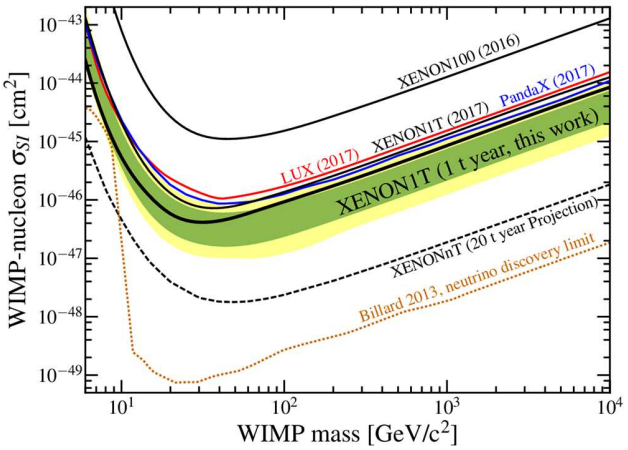

Fig. 5. Results from year-long spin-independent (SI) WIMP-Xe scattering search by Xe-1ton experiment [28] along with results from LUX and PandaX.

Table 1. Upper bounds on sparticle and Higgs boson masses from 10% naturalness using Δ_{BG} within multi-parameter SUSY effective theories, from reference [35] (BG1987) and reference [40] (CGR2009). We also include bounds from Δ_{HS} from references [41,42] (PRW, BKLS2011).

Mass	Upper limit	Source
$m_{\tilde{g}}$	<400 GeV	BG (1987)
$m_{\tilde{u}_R}$	<400 GeV	BG (1987)
$m_{\tilde{e}_R}$	<350 GeV	BG (1987)
$m_{\tilde{\chi}_1^\pm}$	<100 GeV	BG (1987)
$m_{\tilde{\chi}_1^0}$	<50 GeV	BG (1987)
m_h	<115 GeV	CGR (2009)
$m_{\tilde{t}_{1,2},\tilde{b}_1}$	<500 GeV	PRW, BKLS (2011)

also list 10% Δ_{BG} bounds on $m_h < 115$ GeV from reference [40]. For $m_h \sim 125$ GeV, then Δ_{BG} rapidly rises to 1000, or 0.1% fine-tuning. The final entry in Table 1 comes from references [41,42]. Using a different measure (labeled in Sect. 2 as Δ_{HS}), the authors derive that *three* third generation squarks $\tilde{t}_{1,2}$ and $\tilde{b}_1$ should all lie below about 500 GeV. While one third generation squark might hide in Figure 4, it is hard to envision three hiding on the same plot.

Taken all together, the first conclusion from comparing LHC Higgs mass measurements and sparticle mass limits to Table 1, one might draw a rather pessimistic conclusion regarding SUSY. It is that an apparent mass gap has opened up between the weak scale and the sparticle mass scale known as the Little Hierarchy problem (LHP): while SUSY solves the Big Hierarchy problem, a LHP has appeared due to the strong limits from LHC data. The emergence of the LHP has engendered growing skepticism that the common notion of SUSY with weak scale sparticles is nature's solution to the hierarchy problems.

1.5 SUSY: from cartoon to paradigm

In this midi-review (between a mini-review and a review), we will argue that the above pessimistic conclusion is too strong, and is based on an overly simplistic notion of weak scale SUSY that is relatively unchanged since the 1980s. In fact, several

developments have emerged since the year 2000 that have changed the paradigm notion of how SUSY might appear. These include the following.

- Improved scrutiny of the notion of naturalness and naturalness measures shows that many of the early notions of naturalness are in need of revision. In particular, the model independent electroweak measure Δ_{EW} has emerged [43]. Under Δ_{EW}, then a modified SUSY paradigm arises with higgsinos rather than gauginos as the lightest electroweakinos. Under Δ_{EW}, other sparticle mass limits are lifted by factors of 2–50 beyond the early projections from Table 1. This has important consequences for collider searches and for the picture of SUSY dark matter. An updated discussion of naturalness is the topic of Section 2.

- The intertwining of the SUSY μ problem [44], the strong CP problem and the role of the axion in SUSY theories forms the topic of Section 3. The role of discrete R-symmetries [45–47] is discussed which helps to simultaneously solve the SUSY μ problem and proton-decay problem. In addition, both R-parity and the global Peccei-Quinn (PQ) $U(1)_{PQ}$ needed for an axionic solution to the strong CP problem can emerge from the strongest of these, a $\mathbf{Z}_{24}^R$. In this case, then dark matter would be composed of two particles: a mixture of higgsino-like WIMPs and DFSZ-like axions with suppressed couplings to photons.

- Starting in 2001, it was realized that the multitude of string theory vacua [48–50] provided a setting for Weinberg's anthropic solution to the cosmological constant problem [51]. Rather general stringy considerations of the so-called "landscape" of vacua solutions also suggest a statistical preference for *large soft terms* from the multiverse [52]. This stringy statistical draw must be compensated for by requiring that the derived value for the weak scale in each pocket universe of the multiverse be not too far from our measured value, so that complex nuclei and hence atoms arise in any anthropically allowed pocket universe [53,54]. By combining these notions, then it is seen that the Higgs mass $m_h \sim 125$ GeV is statistically favored while sparticle masses are drawn beyond LHC search limits [55]. Under such a *stringy natural* setting, a 3 TeV gluino is more natural than a 300 GeV gluino [56].

We compare the predictions of landscape SUSY sparticle mass spectra to those of several other prominent string phenomenology constructs in Section 5.

After addressing the above issues, then we briefly summarize the conclusions as to how SUSY is likely to arise at LHC upgrades and ILC in Section 6. In Section 7, we summarize expectations for mixed axion/WIMP dark matter and explain why so far no WIMPs have emerged at direct/indirect detection experiments. In Section 8, we briefly summarize several compelling scenarios for baryogenesis in SUSY models. Our overall summary and big picture is presented in Section 9.

2 Naturalness re-examined

In this section, we make a critical assessment of several common naturalness measures found in the literature.[1] We then follow up with revised upper bounds on sparticle masses arising from clarification of electroweak naturalness in SUSY models.

[1]Some recent model scans of Δ_{BG} and Δ_{EW} and associated DM and collider phenomenology can be found in references [57,58].

2.1 Δ_{EW}: electroweak naturalness

The simplest naturalness measure Δ_{EW} [43,59] arises from the form of the Higgs potential in the MSSM. By minimizing the weak-scale SUSY Higgs potential, including radiative corrections, one may relate the measured value of the Z-boson mass to the various SUSY contributions:

$$\begin{aligned} m_Z^2/2 &= \frac{m_{H_d}^2 + \Sigma_d^d - (m_{H_u}^2 + \Sigma_u^u)\tan^2\beta}{\tan^2\beta - 1} - \mu^2 \\ &\simeq -m_{H_u}^2 - \mu^2 - \Sigma_u^u(\tilde{t}_{1,2}). \end{aligned} \tag{4}$$

The measure

$$\Delta_{EW} = |(max\ RHS\ contribution)|/(m_Z^2/2), \tag{5}$$

is then low provided all *weak-scale* contributions to $m_Z^2/2$ are comparable to or less than $m_Z^2/2$, in accord with practical naturalness. The Σ_u^u and Σ_d^d contain over 40 radiative corrections which are listed in the Appendix of reference [59]. The conditions for natural SUSY (for e.g. $\Delta_{EW} < 30$)[2] can then be read off from equation (5):

- The superpotential μ parameter has magnitude not too far from the weak scale, $|\mu| \lesssim 300$ GeV [61–64]. This implies the existence of light higgsinos $\widetilde{\chi}_{1,2}^0$ and $\widetilde{\chi}_1^\pm$ with $m(\widetilde{\chi}_{1,2}^0, \widetilde{\chi}_1^\pm) \sim 100 - 300$ GeV.
- $m_{H_u}^2$ is radiatively driven from large high scale values to *small* negative values at the weak scale (this is SUSY with *radiatively-driven naturalness* or RNS [43]).
- Large cancellations occur in the $\Sigma_u^u(\tilde{t}_{1,2})$ terms for large A_t parameters which then allow for $m_{\tilde{t}_1} \sim 1 - 3$ TeV for $\Delta_{EW} < 30$. The large A_t term gives rise to large mixing in the top-squark sector and thus lifts the Higgs mass m_h into the vicinity of 125 GeV. The gluino contribution to the weak scale is at two-loop order so its mass can range up to $m_{\tilde{g}} \lesssim 6$ TeV with little cost to naturalness [59,60,65].
- Since first/second generation squarks and sleptons contribute to the weak scale at one-loop through (mainly cancelling) D-terms and at two-loops via RGEs, they can range up to 10–30 TeV with little cost to naturalness (thus helping to alleviate the SUSY flavor and CP problems) [66,67].

Since Δ_{EW} is determined by the weak scale SUSY parameters, then different models which give rise to exactly the same sparticle mass spectrum will have the same fine-tuning value (model independence). Using the naturalness measure Δ_{EW}, then it has been shown that plenty of SUSY parameter space remains natural even in the face of LHC Run 2 Higgs mass measurements and sparticle mass limits [59].

2.2 Δ_{HS}: tuning dependent contributions

It is also common in the literature to apply practical naturalness to the Higgs mass:

$$m_h^2 \simeq m_{H_u}^2(weak) + \mu^2(weak) + mixing + rad.\ corr, \tag{6}$$

[2] The onset of finetuning for $\Delta_{EW} \gtrsim 30$ is visually displayed in Figure 1 of reference [60].

where the mixing and radiative corrections are both comparable to m_h^2. Also, in terms of some high energy cut-off scale (HS) Λ, then $m_{H_u}^2(weak) = m_{H_u}^2(\Lambda) + \delta m_{H_u}^2$ where it is common to estimate $\delta m_{H_u}^2$ using its renormalization group equation (RGE) by setting several terms in $dm_{H_u}^2/dt$ (with $t = \log Q^2$) to zero so as to integrate in a single step:

$$\delta m_{H_u}^2 \sim -\frac{3f_t^2}{8\pi^2}(m_{Q_3}^2 + m_{U_3}^2 + A_t^2)\ln\left(\Lambda^2/m_{soft}^2\right). \tag{7}$$

Taking $\Lambda \sim m_{GUT}$ and requiring the high scale measure

$$\Delta_{HS} \equiv \delta m_{H_u}^2/m_h^2. \tag{8}$$

$\Delta_{HS} \lesssim 1$ then requires three third generation squarks lighter than 500 GeV [41,42] (now highly excluded by LHC top-squark searches) and small A_t terms (whereas $m_h \simeq 125$ GeV typically requires large mixing and thus multi-TeV values of A_0 [20, 21,68]). The simplifications made in this calculation ignore the fact that $\delta m_{H_u}^2$ is highly dependent on $m_{H_u}^2(\Lambda)$ (which is set to zero in the simplification) [69–71]. In fact, the larger one makes $m_{H_u}^2(\Lambda)$, then the larger becomes the cancelling correction $\delta m_{H_u}^2$. Thus, these terms are *not independent*: one cannot tune $m_{H_u}^2(\Lambda)$ against a large contribution $\delta m_{H_u}^2$. Thus, weak-scale top squarks and small A_t are not required by naturalness.

2.3 Δ_{BG}: the problem with parameters

The more traditional measure Δ_{BG} was proposed by Ellis et al. [72] and later investigated more thoroughly by Barbieri and Giudice [35]. The starting point is to express m_Z^2 in terms of weak scale SUSY parameters as in equation (5):

$$m_Z^2 \simeq -2m_{H_u}^2 - 2\mu^2, \tag{9}$$

where the partial equality obtains for moderate-to-large $\tan\beta$ values and where we assume for now that the radiative corrections are small. An advantage of Δ_{BG} over the previous large-log measure is that it maintains the correlation between $m_{H_u}^2(\Lambda)$ and $\delta m_{H_u}^2$ by replacing $m_{H_u}^2(m_{weak}) = \left(m_{H_u}^2(\Lambda) + \delta m_{H_u}^2\right)$ by its expression in terms of high scale parameters. To evaluate Δ_{BG}, one needs to know the explicit dependence of $m_{H_u}^2$ and μ^2 on the fundamental parameters. Semi-analytic solutions to the one-loop renormalization group equations for $m_{H_u}^2$ and μ^2 can be found for instance in references [73,74]. For the case of $\tan\beta = 10$, then [75–77]

$$\begin{aligned} m_Z^2 \simeq & -2.18\mu^2 + 3.84M_3^2 + 0.32M_3M_2 + 0.047M_1M_3 \\ & -0.42M_2^2 + 0.011M_2M_1 - 0.012M_1^2 - 0.65M_3A_t \\ & -0.15M_2A_t - 0.025M_1A_t + 0.22A_t^2 + 0.004M_3A_b \\ & -1.27m_{H_u}^2 - 0.053m_{H_d}^2 \\ & +0.73m_{Q_3}^2 + 0.57m_{U_3}^2 + 0.049m_{D_3}^2 - 0.052m_{L_3}^2 + 0.053m_{E_3}^2 \\ & +0.051m_{Q_2}^2 - 0.11m_{U_2}^2 + 0.051m_{D_2}^2 - 0.052m_{L_2}^2 + 0.053m_{E_2}^2 \\ & +0.051m_{Q_1}^2 - 0.11m_{U_1}^2 + 0.051m_{D_1}^2 - 0.052m_{L_1}^2 + 0.053m_{E_1}^2, \end{aligned} \tag{10}$$

where all terms on the right-hand-side are understood to be *GUT* scale parameters.

Table 2. Values of Δ_{BG} for various hypothetical effective SUSY theories leading to the exact same weak scale spectrum. We take $m_0 = 3500$ GeV, $m_{1/2} = 300$ GeV, $A_0 = 0$ and $\tan\beta = 10$ with $\mu = 330.6$ GeV and $m_A = 3468$ GeV. The corresponding value of Δ_{EW} is 32.7. The DDSB stands for the one-soft-parameter ($=m_{3/2}$) dilaton-dominated SUSY breaking model.

Model	Δ_{BG}
nuhm2	984
mSUGRA/CMSSM	41
DDSB($m_{3/2}$)	29.4
pMSSM	28.9

Then, the proposal is that the variation in m_Z^2 with respect to parameter variation be small:

$$\Delta_{BG} \equiv max_i\,[c_i] \quad \text{where} \quad c_i = \left|\frac{\partial \ln m_Z^2}{\partial \ln p_i}\right| = \left|\frac{p_i}{m_Z^2}\frac{\partial m_Z^2}{\partial p_i}\right|, \tag{11}$$

where the p_i constitute the fundamental parameters of the model. Thus, Δ_{BG} measures the fractional change in m_Z^2 due to fractional variation in the high scale parameters p_i. The c_i are known as *sensitivity coefficients* [77].

The requirement of low Δ_{BG} is then equivalent to the requirement of no large cancellations on the right-hand-side of equation (10) since (for linear terms) the logarithmic derivative just picks off coefficients of the relevant parameter. For instance, $c_{m_{Q_3}^2} = 0.73 \cdot (m_{Q_3}^2/m_Z^2)$. If one allows $m_{Q_3} \sim 3$ TeV (in accord with requirements from the measured value of m_h), then one obtains $c_{m_{Q_3}^2} \sim 800$ and so $\Delta_{BG} \geq 800$. In this case, SUSY would be electroweak fine-tuned to about 0.1%. If instead one sets $m_{Q_3} = m_{U_3} = m_{H_u} \equiv m_0$ as in models with scalar mass universality, then the various scalar mass contributions to m_Z^2 largely cancel and $c_{m_0^2} \sim -0.017\ m_0^2/m_Z^2$: the contribution to Δ_{BG} from scalars drops by a factor ∼50.

The above argument illustrates the extreme model-dependence of Δ_{BG} for multi-parameter SUSY models. The value of Δ_{BG} can change radically from theory to theory even if those theories generate exactly the same weak scale sparticle mass spectrum: see Table 2. The model dependence of Δ_{BG} arises due to a violation of the definition of practical naturalness: one must combine dependent terms into independent quantities before evaluating EW fine-tuning [69–71,78].

2.4 Some natural SUSY models: NUHM2, NUHM3, nGMM and nAMSB

A fairly reliable prediction of natural SUSY models is that the four higgsinos $\widetilde{\chi}_1^{\pm}$ and $\widetilde{\chi}_{1,2}^0$ lie at the bottom of the SUSY particle mass spectra with mass values $\sim\mu \lesssim 200 - 300$ GeV. However, even this prediction can be upset by models with non-universal gaugino masses where for instance the gluino is still beyond LHC bounds but where the bino mass M_1 and/or the wino mass M_2 is comparable to or lighter than μ [79]. In addition, there are several theory motivated models which all give rise to natural SUSY spectra with $\Delta_{EW} \lesssim 30$. These include:

– The two- or three- extra parameter non-universal Higgs models, NUHM2 or NUHM3 [80–85]. These models are slight generalizations of the CMSSM/mSUGRA model [36–39] where gaugino masses are unified to $m_{1/2}$ at the GUT scale but where the soft Higgs masses m_{H_u} and m_{H_d} are instead independent of the matter scalar soft masses m_0. This is well justified since the

Higgs superfields necessarily live in different GUT multiplets than the matter superfields. In the NUHM3 model, it is further assumed that the third generation matter scalars are split from the first two generation $m_0(1,2) \neq m_0(3)$. In these models, typically the parameter freedom in m_{H_u} and m_{H_d} is traded for the more convenient weak scale parameters μ and m_A.

– The original minimal anomaly-mediated SUSY breaking model [86–89] (mAMSB) now seems excluded since wino-only dark matter should have been detected by indirect dark matter searches [90–92]. Also, in mAMSB the anomaly-mediated contribution to the trilinear soft term A is usually too small to boost the Higgs mass $m_h \rightarrow 125$ Gev unless stop masses lie in the hundred-TeV range. Finally, the mAMSB model typically has a large μ term. The latter two situations lead to mAMSB being highly unnatural, especially if $m_h \simeq 125$ GeV is required.

  In the original Randall-Sundrum paper, the authors suggest additional bulk contributions to scalar masses to solve the problem of tachyonic sleptons. If the bulk contributions to $m_{H_u}^2$ and $m_{H_d}^2$ are non-universal with the matter scalars, then one can allow for a small natural μ term. Also, if bulk contributions to the A terms are allowed, (as suggested in the Randall-Sundrum paper), then large stop mixing can occur which both reduces the $\Sigma_u^u(\tilde{t}_{1,2})$ terms in equation (5) while lifting $m_h \rightarrow 125$ GeV. In that case, natural AMSB models can be generated with small $\Delta_{EW} < 30$ and with $m_h \simeq 125$ GeV [97]. The phenomenology of *natural* AMSB (nAMSB) is quite different from mAMSB: in nAMSB, the higgsinos are the lightest electroweakinos so one has a higgsino-like LSP even though the winos are still the lightest gauginos. Axions are assumed to make up the bulk of dark matter [98].

– The scheme of mirage-mediation (MM) posits soft SUSY breaking terms which are suppressed compared to the gravitino mass $m_{3/2}$ so that moduli/gravity mediated contributions to soft terms are comparable to AMSB contributions [99–103]. The original MM calculation of soft terms within the context of KKLT moduli stabilization with a single Kähler modulus (stabilized by non-perturbative contributions) in type-IIB string models with D-branes depended on discrete choices for modular weights. These original MM models have been shown to be unnatural under LHC Higgs mass and sparticle limit constraints [70]. However, in more realistic compactifications with many Kähler moduli, then a more general framework where the discrete modular weights are replaced by continuous parameters is called for. The resulting generalized mirage-mediation model (GMM) maintains the phenomena of mirage unification of gaugino masses while allowing the flexibility of generating $m_h \simeq 125$ GeV while maintaining naturalness in the face of LHC sparticle mass limits. In *natural* GMM models (nGMM) [104], the gaugino spectrum is still compressed as in usual MM, but now the higgsinos lie at the bottom of the spectra. Consequently, the collider and dark matter phenomenology is modified from previous expectations. In the nGMM$'$ model, the continuous parameters c_{H_u} and c_{H_d} (which used to depend on discrete modular weights) can be traded as in NUHM2,3 for the more convenient weak scale parameters μ and m_A.

A schematic sketch of the three spectra fron NUHM2, nGMM$'$ and nAMSB is shown in Figure 6. The models are hardwired in the Isajet SUSY spectrum generator Isasugra [105].

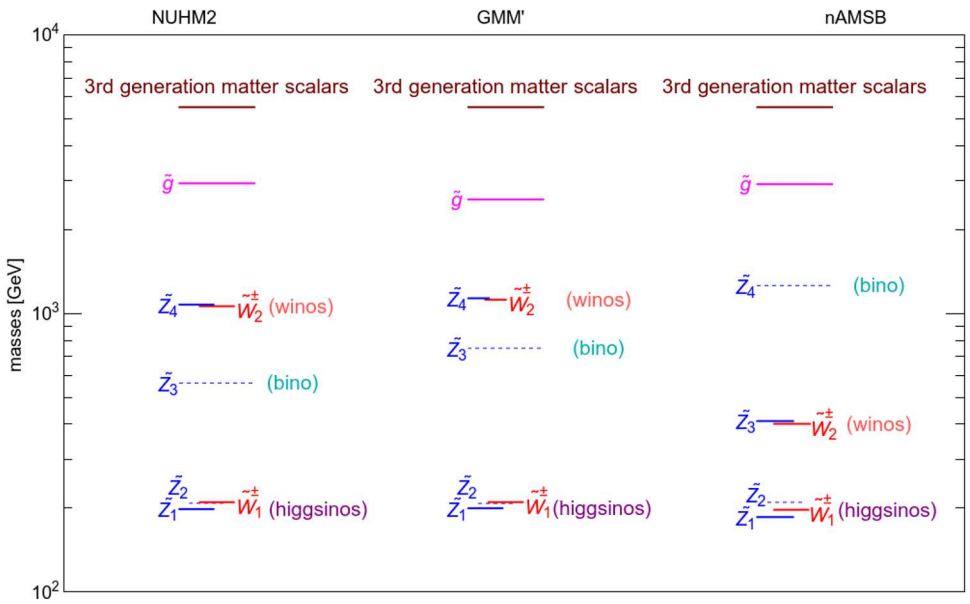

Fig. 6. Typical mass spectra from natural SUSY in the case of NUHM2 (with gaugino mass unification), nGMM with mirage unification and compressed gauginos and natural AMSB where the wino is the lightest gaugino. In all cases, the higgsinos lie at the bottom of the spectra.

2.5 Conclusions on naturalness

In Figure 7, we compare the three aforementioned fine-tuning measures in the m_0 vs. $m_{1/2}$ plane of the mSUGRA/CMSSM model for $A_0 = 0$ and $\tan\beta = 10$. In this plane, the Higgs mass m_h is always well below 125 GeV unless one proceeds to far larger values of m_0 and $m_{1/2}$. Also, the μ parameter is always large except in the HB/FP region near the edge of the right-side "no EWSB" disallowed region. The contour $\Delta_{HS} < 100$ favors the low m_0 and $m_{1/2}$ corner and disallows $m_0 \gtrsim 0.7$ TeV. The BG measure $\Delta_{BG} < 30$ boundary is roughly flat with m_0 variation which shows that heavy squarks, including top-squarks, can still be natural under this measure. The $\Delta_{EW} < 30$ region is denoted by the green contour and is roughly flat with m_0 variation since the contours of fixed μ values (not shown) are also flat with m_0 variation. The curve cuts off around $m_0 \sim 3$ TeV when the radiative corrections $\Sigma_u^u(\tilde{t}_{1,2})$ become large. Note that all measures favor small m_0 and $m_{1/2}$ (in contrast to stringy naturalness introduced in Sect. 4). For comparison, we show the LHC contour $m_{\tilde{g}} = 2.25$ TeV (magenta) where the region below the contour is excluded by LHC gluino pair searches. This picture presents a rather pessimistic view of SUSY. However, one must remember for such parameter choices within the mSUGRA model even the Higgs mass doesn't match its measured value.

In Figure 8, we instead show the various fine-tuning measures in the m_0 vs. $m_{1/2}$ plane but this time in the two-extra-parameter non-universal Higgs model where $m_{H_u}^2$ and $m_{H_d}^2$ are not set to the matter scalar masses m_0. This is sensible since the Higgs multiplets necessarily live in different GUT multiplets than matter scalars. The added parameter freedom always allows for the possibility of small μ parameter since $m_{H_u}^2$ and $m_{H_d}^2$ can be traded for weak scale free parameters μ and m_A via the scalar potential minimization conditions. For this figure, we choose large $A_0 = -1.6m_0$ and $\tan\beta = 10$ but with $\mu = 200$ GeV and $m_A = 2$ TeV. In this case, a wide swath of

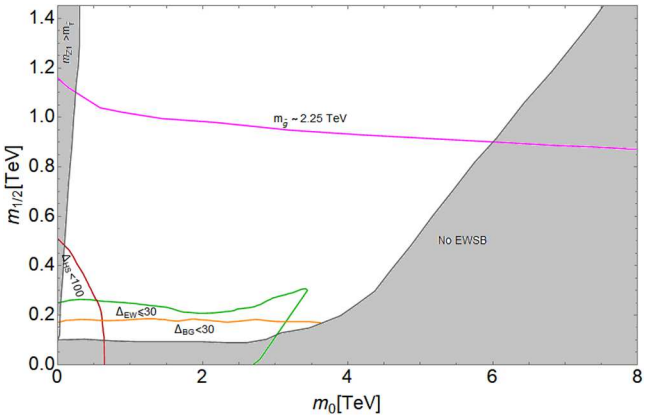

Fig. 7. The m_0 vs. $m_{1/2}$ plane of the mSUGRA/CMSSM model with $A_0 = 0$ and $\tan\beta = 10$. In this parameter space $m_h < 122$ GeV. We show contours of various finetuning measures along with LEP2 and LHC Run 2 search limits (from Ref. [56]).

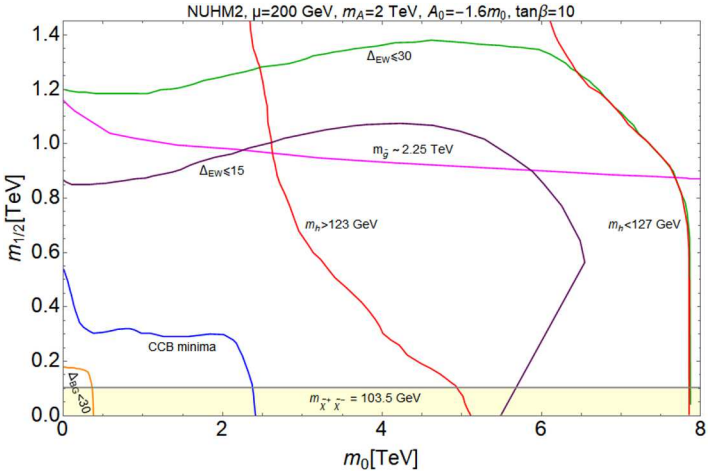

Fig. 8. The m_0 vs. $m_{1/2}$ plane of the NUHM2 model with $A_0 = -1.6m_0$, $\tan\beta = 10$, $\mu = 200$ GeV and $m_A = 2$ TeV. We show contours of various finetuning measures along with Higgs mass contours and LEP2 and LHC Run 2 search limits (from Ref. [56]).

parameter space between the red contours admits a Higgs mass 123 GeV $< m_h <$ 127 GeV in accord with measured values.

In Figure 8, the Δ_{BG} measure is squeezed into the lower-left corner which actually turns out to be a region of charge-and-color breaking (CCB) minima of the Higgs potential. The Δ_{HS} measure cannot be plotted since it would live in the CCB region. However, in this case the $\Delta_{EW} < 30$ contour now appears at very large m_0 and $m_{1/2}$ values (green contour) and extends well beyond the LHC gluino mass limit. Thus, under the model-independent Δ_{EW} measure, plenty of parameter space remains beyond current LHC search limits and with the proper value of light Higgs mass $m_h \sim 125$ GeV. In fact, scans over many SUSY models with $m_h \sim 125$ GeV including mSUGRA/CMSSM, GMSB, AMSB and various mirage mediation models with discrete values of modular weights all turn out to be highly fine-tuned under Δ_{EW} [70]. Thus, these models would be excluded by LHC as being *unnatural* [69].

Table 3. Upper bounds on sparticle masses from 3% naturalness using Δ_{BG} within multi-parameter SUSY effective theories, from references [35,106] to references [60,65].

Mass	BG/DG	Δ_{EW}
μ	<350 GeV	<350 GeV
$m_{\tilde{g}}$	$<400-600$ GeV	<6 TeV
$m_{\tilde{t}_1}$	<450 GeV	<3 TeV
$m_{\tilde{q},\tilde{\ell}}$	$<550-700$ GeV	$<10-30$ TeV

On the other hand, NUHM2 and NUHM3, generalized mirage mediation (with continuous rather than discrete parameters) [104], natural AMSB [97] are all allowed since sizable natural regions of parameter space remain beyond LHC limits and with $m_h \sim 125$ GeV.

By scanning the natural SUSY models over all parameter space and requiring $m_h = 125 \pm 2$ GeV and $\Delta_{EW} < 30$, then new upper bounds can be found for sparticle masses [59,60,65]. These are listed in Table 3 along with the older bounds from references [35,106] with $\Delta_{BG} < 30$. From Table 3, we see that the upper bound on the μ parameter is $\mu < 350$ GeV for both measures. However, the naturalness upper bound on $m_{\tilde{g}}$ has increased from the old value of $m_{\tilde{g}} \lesssim 0.4-0.6$ TeV to the new bound $m_{\tilde{g}} \lesssim 6$ TeV: well beyond present LHC bounds and even well beyond projected search limits for high-luminosity (HL) LHC (which extend to $m_{\tilde{g}} \sim 2.7$ TeV) [107]. The old bounds for top squarks were $m_{\tilde{t}_1} \lesssim 0.45$ TeV, but under Δ_{EW} these extend to $m_{\tilde{t}_1} < 3$ TeV, again well-beyond the reach of HL-LHC. And whereas before first/second generation squarks and sleptons were required to lie $m_{\tilde{q},\tilde{\ell}} < 0.55-0.7$ TeV, now using Δ_{EW} we find $m_{\tilde{q},\tilde{\ell}} \lesssim 10-30$ TeV (allowing for a mixed decoupling/degeneracy solution to the SUSY flavor and CP problems [67]). Thus, we find that under a clarified notion of naturalness, plenty of parameter space for weak scale SUSY remains natural and with $m_h \simeq 125$ GeV.

A pictorial representation of the natural SUSY spectra is shown in Figure 9. Here, we see that four light higgsinos $\widetilde{\chi}^0_{1,2}$ and $\widetilde{\chi}^{\pm}_1$ are at the bottom of the spectra with mass $m(higgsinos) \sim \mu$ and with mass splittings of order $5-15$ GeV: highly compressed. The other gauginos and stops and sbottoms can now live in the multi-TeV region safely beyond current LHC bounds while first/second generation squarks and sleptons inhabit the tens of TeV regime. The LSP is now the lightest higgsino which is very different from older expectations. The natural mass ordering brings in new SUSY search strategies for LHC and new expectations for SUSY dark matter.

3 QCD naturalness, Peccei-Quinn symmetry, the μ problem and discrete symmetries

3.1 QCD naturalness, PQ and axions

While we require naturalness in the electroweak sector, it is important to recall that there is also a naturalness problem in the QCD sector of the SM. In the early days of QCD, it was a mystery why the two-light-quark chiral symmetry $U(2)_L \times U(2)_R$ gave rise to three and not four light pions [108]. The mystery was resolved by 't Hooft's discovery of the QCD theta vacuum which allows for the emergence of three pseudo-Goldstone bosons– the pion triplet– from the spontaneously broken global $SU(2)_{axial}$ symmetry, but that didn't respect the remaining $U(1)_A$ symmetry [109].

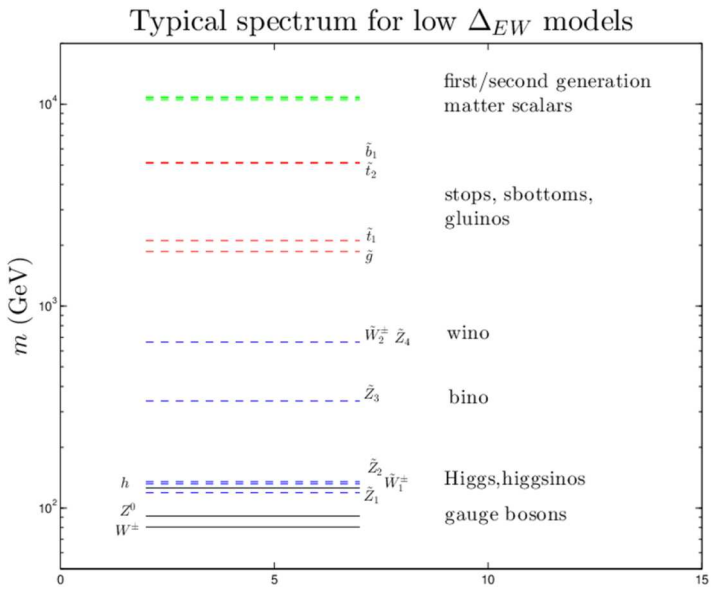

Fig. 9. Typical mass spectra from natural SUSY where four light higgsinos lie at the lowest rungs of the anticipated mass spectra.

As a consequence of the theta vacuum, one expects the presence of a term

$$\mathcal{L} \ni \frac{\bar{\theta}}{32\pi^2} F_{A\mu\nu}\tilde{F}_A^{\mu\nu}, \tag{12}$$

in the QCD Lagrangian (where $\bar{\theta} = \theta + arg(det(\mathcal{M}))$ and $\mathcal{M}$ is the quark mass matrix). Measurements of the neutron EDM constrain $\bar{\theta} \lesssim 10^{-10}$ leading to an enormous fine-tuning in $\bar{\theta}$: the so-called strong CP problem [110]. The strong CP problem is elegantly solved via the PQWW [111–113] introduction of PQ symmetry and the concomitant (invisible [114–117]) axion: the offending term can dynamically settle to zero. The axion a is a valid dark matter candidate in its own right [118–121].

Introducing the axion in a SUSY context solves the strong CP problem but also offers an elegant solution to the SUSY μ problem [122]. The SUSY μ problem consists of two parts. First, the superpotential μ term $W \ni \mu H_u H_d$ is SUSY conserving and so one expects μ of order the Planck scale $\mu \sim m_P$. Thus, it must be at first forbidden, perhaps by some symmetry. Second, the μ term must be generated, perhaps via symmetry breaking, such that μ obtains a natural value of order the weak scale $\mu \sim m_{weak}$. A recent review of twenty solutions to the SUSY μ problem is presented in reference [44].

The most parsimonius implementation of the strong CP solution involves introducing a single MSSM singlet superfield S carrying PQ charge $Q_{PQ} = -1$ while the Higgs fields both carry $Q_{PQ} = +1$. The usual μ term is forbidden by the global $U(1)_{PQ}$ symmetry, but then we have a superpotential [123,124]

$$W_{DFSZ} \ni \lambda \frac{S^2}{m_P} H_u H_d. \tag{13}$$

If PQ symmetry is broken and S receives a VEV $\langle S \rangle \sim f_a$, then a weak scale μ term

$$\mu \sim \lambda f_a^2 / m_P, \tag{14}$$

is induced which gives $\mu \sim m_Z$ for $f_a \sim 10^{10}$ GeV. While Kim-Nilles sought to relate the PQ breaking scale f_a to the hidden sector mass scale m_{hidden} [122], we see now that the Little Hierarchy

$$\mu \sim m_Z \ll m_{3/2} \sim \text{multi} - \text{TeV}, \tag{15}$$

could emerge due to a mis-match between the PQ breaking scale and hidden sector mass scale $f_a \ll m_{hidden}$.

The PQ solution has for long been seen as straddling dangerous ground. The global $U(1)_{PQ}$ at the heart of the PQ solution is understood to be inconsistent with the inclusion of gravity in particle physics [125–132]. If PQ is to work, then the underlying $U(1)_{PQ}$ global symmetry ought to emerge as an accidental, approximate symmetry arising from some more fundamental gravity-safe symmetry, much as baryon and lepton number conservation arise in the SM accidentally as a consequence of the more fundamental gauge symmetry. The fundamental gravity-safe symmetry must be especially sharp: if any PQ violating non-renormalizable terms occur in the PQ sector scalar potential that are suppressed by fewer powers than $(1/m_P)^8$, then they will cause a shift in the vacuum value such that $\bar{\theta} > 10^{-10}$ [130–132].

In addition, other problematic terms may arise in the superpotential. Based upon gauge invariance alone, one expects the MSSM superpotential to be of the form

$$\begin{aligned} W_{MSSM} \ni & \mu H_u H_d + \kappa_i L_i H_u + m_N^{ij} N_i^c N_j^c \\ & + f_e^{ij} L_i H_d E_j^c + f_d^{ij} Q_i H_d D_j^c + f_u^{ij} Q_i H_u U_j^c + f_\nu^{ij} L_i H_u N_j^c \\ & + \lambda_{ijk} L_i L_j E_k^c + \lambda'_{ijk} L_i Q_j D_k^c + \lambda''_{ijk} U_i^c D_j^c D_k^c \\ & + \frac{\kappa_{ijkl}^{(1)}}{m_P} Q_i Q_j Q_k L_l + \frac{\kappa_{ijkl}^{(2)}}{m_P} U_i^c U_j^c D_k^c E_l^c. \end{aligned} \tag{16}$$

The first term on line 1 of equation (16), if unsuppressed, should lead to Planck-scale values of μ while phenomenology (Eq. (5)) requires μ of order the weak scale $\sim$100−350 GeV. The κ_i, λ_{ijk}, λ'_{ijk} and λ''_{ijk} terms violate either baryon number B or lepton number L or both and can, if unsuppressed, lead to rapid proton decay and an unstable lightest SUSY particle (LSP). The $f_{u,d,e}^{ij}$ are the quark and lepton Yukawa couplings and must be allowed to give the SM fermions mass via the Higgs mechanism. The $\kappa_{ijkl}^{(1,2)}$ terms lead to dimension-five proton decay operators and are required to be either highly suppressed or forbidden.

It is common to implement discrete symmetries to forbid the offending terms and allow the required terms in equation (16). For instance, the $\mathbf{Z}_2^M$ matter parity (or R-parity) forbids the κ_i and $\lambda_{ijk}^{(\prime,\prime\prime)}$ terms but allows for μ and the $\kappa_{ijkl}^{(1,2)}$ terms: thus, the ad-hoc R-parity conservation all by itself is insufficient to cure all of the ills of equation (16)

One way to deal with the gravity spoliation issue is to assume instead a gravity-safe discrete gauge symmetry $\mathbf{Z}_M$ of order M. The $\mathbf{Z}_M$ discrete gauge symmetry can forbid the offending terms of equation (16) while allowing the necessary terms [133]. Babu, Gogoladze and Wang [134] have proposed a model (written previously by Martin [135–137] thus labelled MBGW) with

$$W_{MBGW} \ni \lambda_\mu \frac{X^2 H_u H_d}{m_P} + \lambda_2 \frac{(XY)^2}{m_P}, \tag{17}$$

which is invariant under a $\mathbf{Z}_{22}$ discrete gauge symmetry. These $\mathbf{Z}_{22}$ charge assignments have been shown to be anomaly-free under the presence of a Green-Schwarz (GS)

Table 4. PQ charge assignments for various superfields of the MBGW and GSPQ (hybrid CCK) models of PQ breaking from SUSY breaking. Another gravity-safe (hybrid SPM) model will have the same PQ charges as GSPQ except $Q(X) = -1/3$ and $Q(Y) = 1$.

Multiplet	MBGW	GSPQ
H_u	-1	-1
H_d	-1	-1
Q	1	1
L	1	1
U^c	0	0
D^c	0	0
E^c	0	0
N^c	0	0
X	1	1
Y	-1	-3

term [138] in the anomaly cancellation calculation. The PQ symmetry then arises as an *accidental approximate global symmetry* as a consequence of the more fundamental discrete gauge symmetry. The PQ charges of the MBGW model are listed in Table 4. The discrete gauge symmetry $\mathbf{Z}_M$ might arise if a charge $Q = Me$ field condenses and is integrated out of the low energy theory while charge e fields survive (see Krauss and Wilczek, Refs. [139–141]). While the ensuing low energy theory should be gravity safe, for the case at hand one might wonder at the plausibility of a condensation of a charge 22 object and whether it might occupy the so-called *swampland* [142] of theories not consistent with a UV completion in string theory. In addition, the charge assignments [134] are not consistent with $SU(5)$ or $SO(10)$ grand unification which may be expected at some level in a more ultimate theory. Beside the terms in equation (17), the lowest order PQ-violating term in the superpotential is $\frac{(Y)^{11}}{m_P^8}$: thus the MBGW model is gravity safe.

An alternative very compelling approach is to implement a discrete R symmetry $\mathbf{Z}_N^R$ of order N.[3] Such discrete R symmetries are expected to arise as discrete remnants from compactification of 10-d (Lorentz symmetric) spacetime down to 4-dimensions [146,147] and thus should be in themselves gravity safe [148]. In fact, in Lee et al. [149], it was found that the requirement of an anomaly-free discrete symmetry that forbids the μ term and all dimension four- and five- baryon and lepton number violating terms in equation (16) while allowing the Weinberg operator LH_uLH_u and that commutes with $SO(10)$ (as is suggested by the unification of each family into the 16 of $SO(10)$) has a unique solution: a $\mathbf{Z}_4^R$ R-symmetry. If the requirement of commutation with $SO(10)$ is weakened to commutation with $SU(5)$, then further discrete $\mathbf{Z}_N^R$ symmetries with N being an integral divisor of 24 are allowed [45–47]: $N = 4, 6, 8, 12$ and 24. Even earlier [150], the $\mathbf{Z}_4^R$ was found to be the simplest discrete R-symmetry to realize R-parity conservation whilst forbidding the μ term. In that reference, the μ term was regenerated using Giudice-Masiero [151] which would generate $\mu \sim m_{soft}$ (too large).

R-symmetries are characterized by the fact that superspace co-ordinates θ carry non-trivial R-charge: in the simplest case, $Q_R(\theta) = +1$ so that $Q_R(d^2\theta) = -2$. For the Lagrangian $\mathcal{L} \ni \int d^2\theta W$ to be invariant under R-symmetry, then the superpotential W must carry $Q_R(W) = 2$. The $\mathbf{Z}_N^R$ symmetry gives rise to a universal gauge anomaly ρ mod η where the remaining contribution ρ is cancelled by the Green-Schwarz axio-dilaton shift and $\eta = N$ $(N/2)$ for N odd (even). The anomaly free R

[3] Discrete R symmetries were used in regard to the μ problem in references [143,144] and for the PQ problem in reference [145].

Table 5. Derived MSSM field R charge assignments for various anomaly-free discrete $\mathbf{Z}_N^R$ symmetries which are consistent with $SU(5)$ or $SO(10)$ unification (from Lee et al. [45–47]).

Multiplet	$\mathbf{Z}_4^R$	$\mathbf{Z}_6^R$	$\mathbf{Z}_8^R$	$\mathbf{Z}_{12}^R$	$\mathbf{Z}_{24}^R$
H_u	0	4	0	4	16
H_d	0	0	4	0	12
Q	1	5	1	5	5
U^c	1	5	1	5	5
E^c	1	5	1	5	5
L	1	3	5	9	9
D^c	1	3	5	9	9
N^c	1	1	5	1	1

charges of various MSSM fields are listed in Table 5 for N values consistent with grand unification.

In reference [152], it has been examined whether or not three models–CCK [153], MSY [154,155] and SPM [135–137]– with radiative PQ breaking which also leads to generation of the Majorana neutrino see-saw mass scale M_N can be derived from any of the fundamental $\mathbf{Z}_N^R$ symmetries in Table 5. In almost all cases, the hXN^cN^c operator is disallowed: then there is no large Yukawa coupling present to drive the PQ soft term m_X^2 negative so that PQ symmetry is broken. And since the PQ symmetry does not allow for a Majorana mass term $M_N N^c N^c$, then no see-saw scale can be developed. The remaining cases that did allow for a Majorana mass scale were all found to be not gravity safe. Also, the MBGW model was found to not be gravity safe under any of the $\mathbf{Z}_N^R$ discrete R-symmetries of Table 5.

Next, a hybrid approach between the radiative breaking models and the MBGW model was created by writing a superpotential:

$$\begin{aligned} W \ni\ & f_u Q H_u U^c + f_d Q H_d D^c + f_\ell L H_d E^c \\ & + f_\nu L H_u N^c + f X^3 Y/m_P \\ & + \lambda_\mu X^2 H_u H_d/m_P + M_N N^c N^c/2, \end{aligned} \tag{18}$$

along with PQ charge assignments given under the GSPQ (gravity-safe PQ model) heading of Table 4. For this model, we have checked that there is gravity spoliation for $N = 4,\ 6,\ 8$ and 12. But for $\mathbf{Z}_{24}^R$ and under R-charge assignments $Q_R(X) = -1$ and $Q_R(Y) = 5$, then the lowest order PQ violating superpotential operators allowed are X^8Y^2/m_P^7, Y^{10}/m_P^7 and X^4Y^6/m_P^7. These operators[4] lead to PQ breaking terms in the scalar potential suppressed by powers of $(1/m_P)^8$. For instance, the term $\lambda_3 X^8 Y^2/m_P^7$ leads to $V_{PQ} \ni 24 f\lambda_3^* X^2 Y X^{*7} Y^{*2}/m_P^8 + h.c.$ which is sufficiently suppressed by enough powers of m_P so as to be gravity safe [130–132]. We have also checked that hybrid model using the MSY XYH_uH_d/m_P term is not gravity-safe under any of the discrete R-symmetries of Table 5 but the hybrid SPM model with $Y^2 H_u H_d/m_P$ and charges $Q_R(X) = 5$ and $Q_R(Y) = -13$ is gravity-safe under only $\mathbf{Z}_{24}^R$.

The scalar potential $V_F = |3f\phi_X^2\phi_Y/m_P|^2 + |f\phi_X^3/m_P|^2$ of the hybrid CCK model was augmented by the following soft breaking terms

$$V_{soft} \ni m_X^2|\phi_X|^2 + m_Y^2|\phi_Y|^2 + (f A_f \phi_X^3 \phi_Y/m_P + h.c.), \tag{19}$$

and the resultant scalar potential was minimized. The minimization conditions are the same as those found in reference [155] equations (17)–(18). In the case of the

[4]The X^8Y^2/m_P^7 term was noted previously in references [45–47].

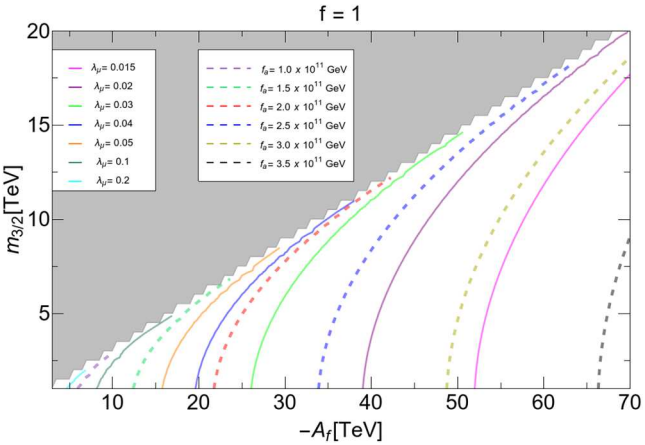

Fig. 10. Representative values of λ_μ required for $\mu = 150$ GeV in the $m_{3/2}$ vs. $-A_f$ plane of the GSPQ model for $f = 1$. We also show several contours of f_a (from Ref. [152]).

GSPQ model, the PQ symmetry isn't broken radiatively, but instead can be broken by adopting a sufficiently large negative value of A_f (assuming real positive couplings for simplicity). The scalar potential admits a non-zero minimum in the fields ϕ_X and ϕ_Y for $A_f < 0$ (see Fig. 1 of reference [152] which is plotted for the case of $m_X = m_Y \equiv m_{3/2} = 10$ TeV, $f = 1$ and $A_f = -35.5$ TeV). For these values, it is found that $v_X = 10^{11}$ GeV, $v_Y = 5.8 \times 10^{10}$ GeV, $v_{PQ} = 1.15 \times 10^{11}$ GeV and $f_a = \sqrt{v_X^2 + 9v_Y^2} = 2 \times 10^{11}$ GeV. These sorts of numerical values lie within the mixed axion/higgsino dark matter sweet spot of cosmologically allowed values and typically give dominant DFSZ axion CDM with ∼10% WIMP dark matter [156–158]. Under these conditions, the model develops a μ parameter $\mu = \lambda_\mu v_X^2/m_P$ and for a value $\lambda_\mu = 0.036$ then we obtain a natural value of the μ parameter at 150 GeV.

The allowed range of GSPQ model parameter space is shown in Figure 10 where we show contours of λ_μ values which lead to $\mu = 150$ GeV in the $m_{3/2}$ vs. $-A_f$ plane for $f = 1$. We also show several representative contours of f_a values. Values of $\lambda_\mu \sim 0.015{-}0.2$ are generally sufficient for a natural μ term and are easily consistent with soft mass $m_{soft} \sim m_{3/2} \sim 2{-}30$ TeV as indicated by LHC searches. We also note that for $m_{3/2} \sim 5{-}20$ TeV, then $f_a \sim 10^{11}$ GeV. Such high values of $m_{3/2}$ also allow for a resolution of the early universe gravitino problem [159,160] (at higher masses gravitinos may decay before the onset of big bang nucleosynthesis (BBN)) and such high soft masses serve to ameliorate the SUSY flavor and CP problems as well [67,161,162]. They are also expected in several well-known string phenomenology constructions including compactification of M-theory on a manifold of G_2 holonomy [163], the minilandscape of heterotic strings compactified on orbifolds [164,165] and the statistical analysis of the landscape of IIB intersecting D-brane models [55].

Thus, the gravity-safe $\mathbf{Z}_{24}^R$ symmetry [45–47] (which may emerge as a remnant of 10-d Lorentz symmetry which is compactified to four spacetime dimensions) yields an accidental approximate global PQ symmetry as implemented in the GSPQ model of PQ symmetry breaking as a consequence of SUSY breaking. The $\mathbf{Z}_{24}^R$ (PQ) symmetry breaking leads to $\mu \ll m_{soft}$ as required by electroweak naturalness and to PQ energy scales $f_a \sim 10^{11}$ GeV as required by mixed axion-higgsino dark matter. The $\mathbf{Z}_{24}^R$ symmetry also forbids the dangerous dimension-four R-parity violating terms. Dimension-five proton decay operators are suppressed to levels well below experimental constraints [45–47]. Overall, the results of reference [152] show that

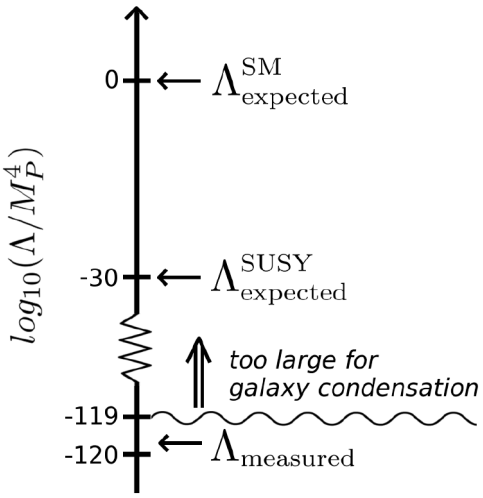

Fig. 11. Log portrayal of expected parameter space of the cosmological constant Λ from the string theory landscape.

the axionic solution to the strong CP problem is enhanced by the presence of both supersymmetry and extra spacetime dimensions which give rise to the gravity-safe $\mathbf{Z}_{24}^R$ symmetry from which the required global PQ symmetry accidentally emerges. It is rather amusing then that both the global $U(1)_{PQ}$ and R-parity emerge from a single more fundamental discrete $\mathbf{Z}_{24}^R$ symmetry.

4 The string landscape and SUSY

In Section 2 we were concerned with naturalness of the EW scale while in Section 3 we were concerned with QCD naturalness involving the CP-violating $\bar{\theta}$ term. If gravity is included in the SM, then a third naturalness problem emerges: why is the vacuum energy density ρ_{vac} so tiny, or alternatively, why is the cosmological constant (CC) Λ so tiny when there is no known symmetry to suppress its magnitude? Naively, one would expect $\Lambda \sim m_P^4$.

At present, the only plausible solution to the CC problem is the hypothesis of the landscape: that a vast number of string theory vacua states exist, each with differing values of physical constants, including Λ. Here, our universe is then just one *pocket universe* present in a vast ensemble of bubble universes contained within the *multiverse*. In this case, a non-zero value of the CC should be present in each pocket universe, but if its value is too large, then the universe would expand too quickly to allow for galaxy condensation and consequently no complex structure would arise, and no observors would be present to measure Λ. This "anthropic" explanation for the magnitude of Λ met with great success by Weinberg who was able to predict its value to within a factor of several well before it was actually measured. The situation is portrayed in Figure 11 where it is anticipated that within a *fertile patch* of the multiverse (all pocket universes containing the SM as the low energy effective theory but with differing values of Λ spread uniformly across the decades of possible values), the value of Λ is about as large as possible such as to give a livable pocket universe.

Can similar reasoning be used to explain the magnitude of other mass scales that appear in theories like the SM or the MSSM? Agrawal et al. [53,54] already examined this question for the case of the magnitude of the weak scale of the SM in 1997.

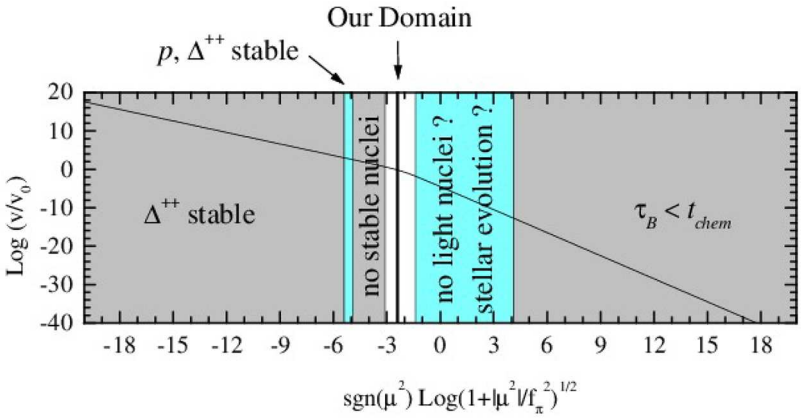

Fig. 12. Allowed values of m_{weak}^{PU} from Agrawal et al. [53,54].

What they found, as depicted in their Figure 12, was that if $m_{weak} \sim m_{W,Z,h}$ of a pocket universe (PU) was larger than our universe's (OU) measured value by a factor $m_{weak}^{PU} \gtrsim (2{-}5)m_{weak}^{OU}$, then weak interactions would become too weak and stable nuclei would all be Δ^{++} baryons: nuclear physics would not be as we know it, and complex nuclei and consequently atoms wouldn't form. This violates the so-called *atomic principle*: that atoms as in our pocket universe must be present for observors such as ourselves to arise.

The emergence of the string theory landscape [48–50] led Douglas [52] to consider whether the scale of SUSY breaking might arise in a similar fashion. In the landscape, then of order 10^{500} different vacua states might exist [166], each with different matter content, gauge groups and physical constants. For a fertile patch of the landscape conatining the MSSM as the low energy effective theory, then the differential distribution of vacua with respect to the hidden sector SUSY breaking scale $m_{hidden}^4 = \sum_i |F_i|^2 + \frac{1}{2}\sum_\alpha D_\alpha^2$ is expected to be of the form

$$dN_{vac}[m_{hidden}^2, m_{weak}, \Lambda] = f_{SUSY}(m_{hidden}^2) \cdot f_{EWSB} \cdot f_{cc} \cdot dm_{hidden}^2, \tag{20}$$

where the soft SUSY breaking scale $m_{soft} \sim m_{3/2} \sim m_{hidden}^2/m_P$. In string theory, it is expected that a number of hidden sectors occur with the overall SUSY breaking scale determined by contributions from various F_i and D_α SUSY breaking fields with non-zero SUSY breaking vevs. The CC is given here by

$$\Lambda = m_{hidden}^4 - 3e^{K/m_P^2}|W|^2/m_P^2, \tag{21}$$

where we assume gravity-mediated SUSY breaking and where K is the Kähler potential and W is the superpotential. A small cosmological constant $\Lambda \sim 0$ can be selected for by scanning over W values distributed uniformly as a complex variable independent of the values of F_i and D_α and hence a small CC has no effect on the distribution of SUSY breaking scales [52,167,168].

Another key observation from examining flux vacua in IIB string theory is that the SUSY breaking F_i and D_α terms are likely to be uniformly distributed– in the former case as complex numbers while in the latter case as real numbers. In this case, one then obtains the following distribution of supersymmetry breaking scales

$$f_{SUSY}(m_{hidden}^2) \sim (m_{hidden}^2)^{2n_F+n_D-1}, \tag{22}$$

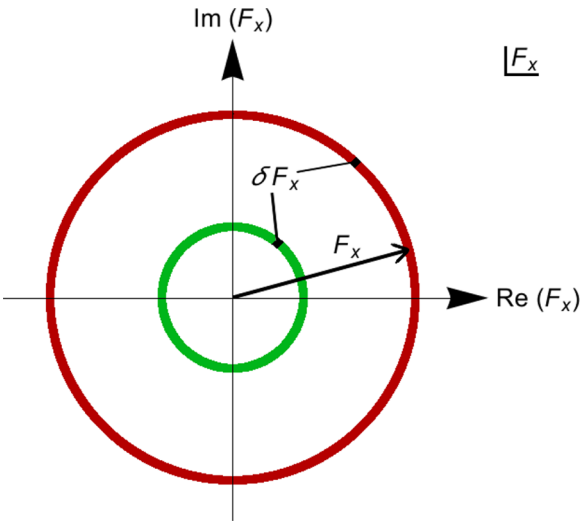

Fig. 13. Annuli of the complex F_X plane giving rise to linearly increasing selection of soft SUSY breaking terms.

where n_F is the number of F-breaking fields and n_D is the number of D-breaking fields in the hidden sector [52]. The case of $n_F = 1$ is displayed in Figure 13. We label the visible sector soft term mass scale as m_{soft} where in SUGRA breaking models we typically have $m_{soft} \sim m_{hidden}^2/m_P \sim m_{3/2}$. Thus, the case of $n_F = 1$ $n_D = 0$ would give a *linearly increasing* probability distribution for generic soft breaking terms simply because the area of annuli within the complex plane increases linearly. We will denote the collective exponent in equation (22) as $n \equiv 2n_F + n_D - 1$ so that the case $n_F = 1$, $n_D = 0$ leads to $n = 1$ with $f_{SUSY}(m_{soft}) \sim m_{soft}^1$. The case $n_F = 0$ with $n_D = 1$ would lead to a uniform distribution in soft terms $f_{SUSY}(m_{soft}) \sim m_{soft}^0$. For the more general case with an assortment of F and D terms contributing comparably to SUSY breaking, then high scale SUSY breaking models would be increasingly favored.

An initial guess for f_{EWFT}– the (anthropic) finetuning factor– was m_{weak}^2/m_{soft}^2 which would penalize soft terms which were much bigger than the weak scale. This ansatz fails on several points.

- Many soft SUSY breaking choices will land one into charge-or-color breaking (CCB) minima of the EW scalar potential. Such vacua would likely not lead to a livable universe and should be vetoed.
- Other choices for soft terms may not even lead to EW symmetry breaking (EWSB). For instance, if $m_{H_u}^2(\Lambda)$ is too large, then it will not be driven negative to trigger spontaneous EWSB (see Fig. 14). These possibilities also should be vetoed.
- In the event of appropriate EWSB minima, then sometimes *larger* high scale soft terms lead to *more natural* weak scale soft terms. For instance, if $m_{H_u}^2(\Lambda)$ is large enough that EWSB is *barely broken*, then $|m_{H_u}^2(weak)| \sim m_{weak}^2$. Likewise, if the trilinear soft breaking term A_t is big enough, then there is large top squark mixing and the $\Sigma_u^u(\tilde{t}_{1,2})$ terms enjoy large cancellations, rendering them $\sim m_{weak}^2$. The same large A_t values lift the Higgs mass m_h up to the 125 GeV regime.

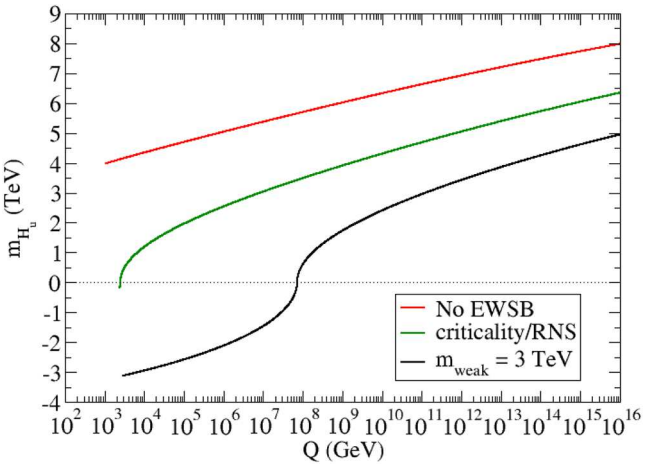

Fig. 14. Evolution of the soft SUSY breaking mass squared term $sign(m_{H_u}^2)\sqrt{|m_{H_u}^2|}$ vs. Q for the case of no EWSB (upper), criticality (middle) as in radiatively-driven natural SUSY (RNS) and $m_{weak} \sim 3$ TeV (lower). Most parameters are the same as in Figure 17.

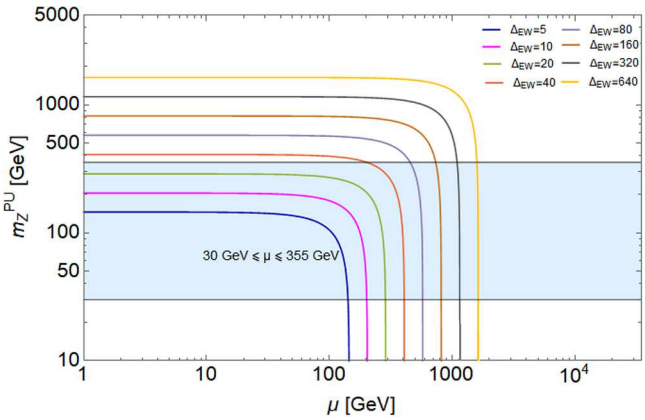

Fig. 15. The pocket universe value of m_Z^{PU} versus the SUSY μ parameter for various values of EW finetuning parameter Δ_{EW}. The anthropic band is shown in blue.

Here, we will assume a *natural* solution to the SUSY μ problem [44]. As seen in Figure 15, a natural value of μ allows for far more landscape vacua to generate an anthropically-required value for m_{weak}. But once μ is fixed, then we are no longer allowed to use it to tune to our measured value of m_Z^{OU}: instead, we must live with the value of m_Z^{PU} generated in each pocket-universe.

Some attractive possibilities for generating μ are the hybrid CCK or SPM models [152] which are based on the previously-mentioned $\mathbf{Z}_{24}^R$ discrete R symmetry which can emerge from compactification of extra dimensions in string theory. The $\mathbf{Z}_{24}^R$ symmetry is strong enough to allow a gravity-safe $U(1)_{PQ}$ symmetry to emerge (which solves the strong CP problem) while also forbidding R-parity violating (RPV) terms (so that WIMP dark matter is generated). Thus, both Peccei-Quinn (PQ) and R-parity conservation (RPC) arise as approximate accidental symmetries similar to the way baryon and lepton number conservation emerge accidentally (and likely approximately) due to the SM gauge symmetries. These hybrid models also solve the SUSY μ

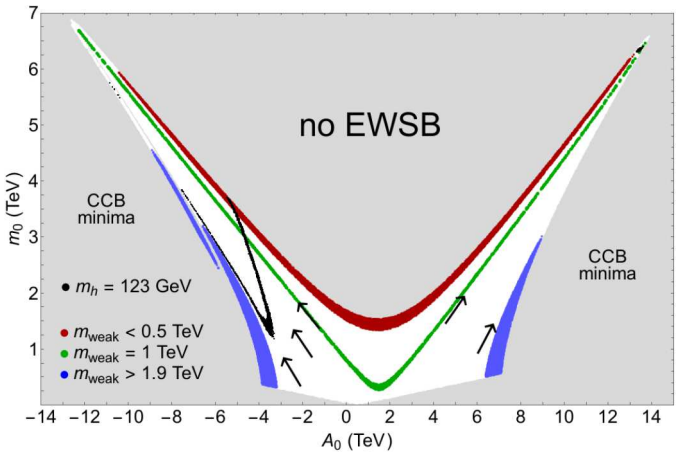

Fig. 16. Contours of m_{weak} in the A_0 vs. m_0 plane for $m_{1/2} = 1$ TeV, $m_{H_u} = 1.3m_0$, $\tan\beta = 10$ and $m_{H_d} = 1$ TeV. The arrows show the direction of statistical/anthropic pull on soft SUSY breaking terms. Within the black contour is where $m_h > 123$ GeV. There is also a slight black contour in the upper-right horn as well.

problem via a Kim-Nilles [122] operator so that $\mu \sim \lambda_\mu f_a^2/m_P$ and $\mu \sim 100{-}200$ GeV (natural) for $f_a \sim 10^{11}$ GeV (the sweet zone for axion dark matter). The $\mathbf{Z}_{24}^R$ symmetry also suppresses dimension-5 proton decay operators [45–47].

Once a natural value of $\mu \sim 100{-}300$ GeV is obtained, then we may invert the usual usage of equation (5) to determine the value of the weak scale in various pocket universes (with MSSM as low energy effective theory) for a given choice of soft terms. Based on nuclear physics calculations by Agrawal et al. [53,54], a pocket universe value of m_{weak}^{PU} which deviates from our measured value by a factor 2–5 is likely to lead to an unlivable universe as we understand it. Weak interactions and fusion processes would be highly suppressed and even complex nuclei could not form. We will adopt a conservative value where the m_{weak}^{PU} should not deviate by more than a factor four from m_{weak}^{OU}. This corresponds to a value of $\Delta_{EW} \lesssim 30$. Thus, for our final form of f_{EWSB} we will adopt

$$f_{EWSB} = \Theta(30 - \Delta_{EW}), \tag{23}$$

while also vetoing CCB or no EWSB vacua.

In Figure 16 we show the A_0 vs. m_0 plane for the NUHM2 model with $m_{1/2}$ fixed at 1 TeV, $\tan\beta = 10$ and $m_{H_d} = 1$ TeV. We take $m_{H_u} = 1.3m_0$. The plane is qualitatively similar for different reasonable parameter choices. We expect A_0 and m_0 statistically to be drawn as large as possible while also being anthropically drawn towards $m_{weak} \sim 100{-}200$ GeV, labelled as the red region where $m_{weak} < 500$ GeV. The blue region has $m_{weak} > 1.9$ TeV and the green contour labels $m_{weak} = 1$ TeV. The arrows denote the combined statistical/anthropic pull on the soft terms: towards large soft terms but low m_{weak}. The black contour denotes $m_h = 123$ GeV with the regions to the upper left (or upper right, barely visible) containing larger values of m_h. We see that the combined pull on soft terms brings us to the region where $m_h \sim 125$ GeV is generated. This region is characterized by highly mixed TeV-scale top squarks [20,21,68]. If instead A_0 is pulled too large, then the stop soft term $m_{U_3}^2$ is driven tachyonic resulting in charge and color breaking minima in the scalar potential (labelled CCB). If m_0 is pulled too high for fixed A_0, then electroweak symmetry isn't even broken.

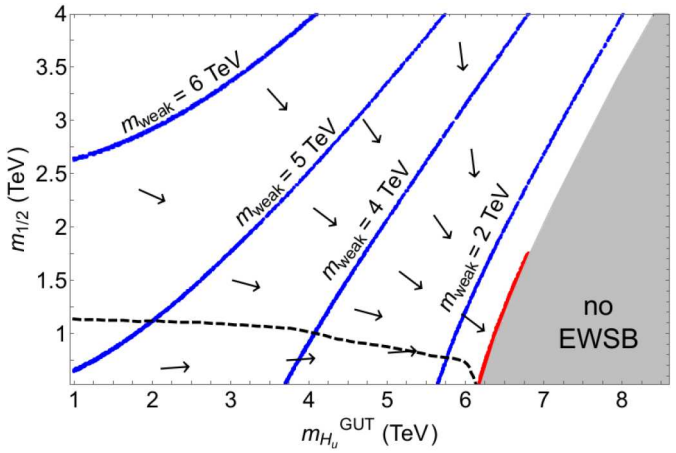

Fig. 17. Contours of m_{weak} (blue) in the m_{H_u} vs. $m_{1/2}$ plane for $m_0 = 5$ TeV, $A_0 = -8$ TeV, $\tan\beta = 10$ and $m_{H_d} = 1$ TeV. Above the black dashed contour is where $m_h > 124$ GeV. The red region has $m_{weak} < 0.5$ TeV. The arrows show the direction of the statistical/anthropic pull on soft SUSY breaking terms.

In Figure 17, we show contours of m_{weak} in the m_{H_u} vs. $m_{1/2}$ plane for $m_0 = 5$ TeV, $A_0 = -8$ TeV, $\tan\beta = 10$ and $m_{H_d} = 1$ TeV. The statistical flow is to large values of soft terms but the anthropic flow is towards the red region where $m_{weak} < 0.5$ TeV. While $m_{1/2}$ is statistically drawn to large values, if it is too large then, as before, the $\tilde{t}_{1,2}$ become too heavy and the $\Sigma_u^u(\tilde{t}_{1,2})$ become too large so that m_{weak} becomes huge. The arrows denote the direction of the combined statistical/anthropic flow. The region above the black dashed contour has $m_h > 124$ GeV. The value of $m_{H_u}(GUT)$ would like to be statistically as large as possible but if it is too large then EW symmetry will not break. Likewise, if $m_{H_u}(GUT)$ is not large enough, then it is driven to large negative values so that $m_{weak} \sim$ the TeV regime and weak interactions are too weak. The situation is shown in Figure 14 where we show the running of $sign(m_{H_u}^2)\sqrt{|m_{H_u}^2|}$ versus energy scale Q for several values of $m_{H_u}^2(GUT)$ for $m_{1/2} = 1$ TeV and with other parameters the same as Figure 17. Too small a value of $m_{H_u}^2(GUT)$ leads to too large a weak scale while too large a value results in no EWSB. The combined statistical/anthropic pull is for *barely-broken* EW symmetry where soft terms teeter on the edge of criticality: between breaking and not breaking EW symmetry. This yields the other naturalness condition that m_{H_u} is driven small negative: then the weak interactions are of the necessary strength. These are just the same conditions for supersymmetric models with radiatively-driven natural SUSY (RNS) [43,59]. Such behavior is termed by reference [169] as *living dangerously* in that the landscape statistically pulls parameters towards the edge– (but not all the way) of disaster.[5]

4.1 Probability distributions for Higgs and sparticle masses from the landscape

To gain numerical predictions for Higgs boson and sparticle masses from the string landscape, we scan over the parameter space of the NUHM3 model with parameters

$$m_0(1,2),\ m_0(3),\ m_{1/2},\ A_0,\ \tan\beta,\ \mu,\ \text{and}\ m_A\ \ (NUHM3), \tag{24}$$

[5]See also Giudice and Rattazzi, reference [170].

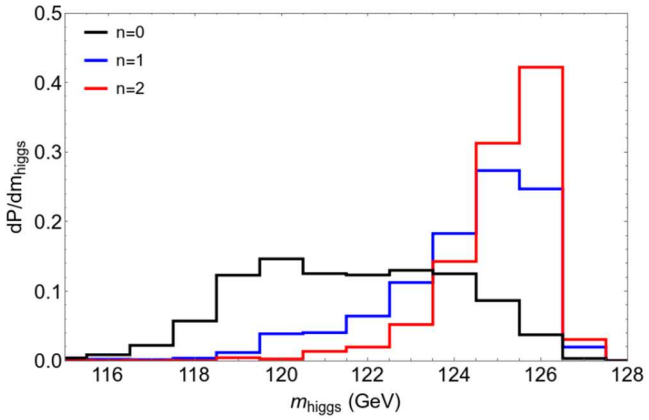

Fig. 18. Distribution in m_h after requiring the anthropic selection of $m_{weak} < 350$ GeV.

with μ fixed at a natural value 150 GeV (which arises from an assumed natural solution to the SUSY μ problem) and a power law selection on soft terms for $n = 0$, 1 and 2. $\tan\beta$ is scanned as flat from 3 to 60.

In Figure 18, we show the landscape probability distribution dP/dm_h vs. m_h for various n values. For $n = 0$, we find a broad spread of values ranging from $m_h \sim 119{-}125$ GeV. This may be expected for the $n = 0$ case since we have a uniform scan in soft terms and low $\Delta_{\rm EW}$ can be found for $A_0 \sim 0$ which leads to little mixing in the stop sector and hence too light values of m_h. Taking $n = 1$, instead we now see that the distribution in m_h peaks at ∼125 GeV with the bulk of probability between 123 GeV $< m_h <$127 GeV– in solid agreement with the measured value of $m_h = 125.09 \pm 0.24$ GeV [171].[6] This may not be surprising since the landscape is pulling the various soft terms towards large values including large mixing in the Higgs sector which lifts up m_h into the 125 GeV range. By requiring the $\Sigma_u^u(\tilde{t}_{1,2})/(m_Z^2/2) \lesssim 30$ (which would otherwise yield a weak scale in excess of 350 GeV) then too large of Higgs masses are vetoed. For the $n = 2$ case with a stronger draw towards large soft terms, the m_h distribution hardens with a peak at $m_h \sim 126$ GeV.

In Figure 19, we show the distribution in gluino mass $m_{\tilde{g}}$. From the figure, we see that the $n = 1$ distribution rises to a peak probability around $m_{\tilde{g}} = 3.5$ TeV. This may be compared to current LHC13 limits which require $m_{\tilde{g}} \gtrsim 2.2$ TeV [174]. Thus, it appears LHC13 has *only begun* to explore the relevant string theory predicted mass values. The distribution fall steadily such that essentially no probability exists for $m_{\tilde{g}} \gtrsim 6$ TeV. This is because such heavy gluino masses lift the top-squark sector soft terms under RG running so that $\Sigma_u^u(\tilde{t}_{1,2})/(m_Z^2/2)$ then exceeds 30. For $n = 2$, the distribution is somewhat harder, peaking at around $m_{\tilde{g}} \sim 4.5$ TeV. The uniform $n = 0$ distribution peaks around 2 TeV.

In Figure 20, we show the probability distribution in $m_{\tilde{t}_1}$. In this case, all three n values lead to a peak around $m_{\tilde{t}_1} \sim 1.5$ TeV. While this may seem surprising at first, in the case of $n = 1,\ 2$ we gain large A_t trilinear terms which lead to large mixing and a diminution of the eigenvalue $m_{\tilde{t}_1}$ [43] even though the soft terms entering the stop mass matrix may be increasing. There is not so much probability below $m_{\tilde{t}_1} = 1$ TeV which corresponds to recent LHC13 mass limits [174,175]. Thus, again, LHC13 has only begun to explore the predicted string theory parameter space. The distributions

[6] Here, we rely on the Isajet 7.87 theory evaluation of m_h which includes renormalization group improved 1-loop corrections to m_h along with leading two-loop effects. Calculated values of m_h are typically within 1−2 GeV of similar calculations from the latest FeynHiggs [172] and SUSYHD [173] codes.

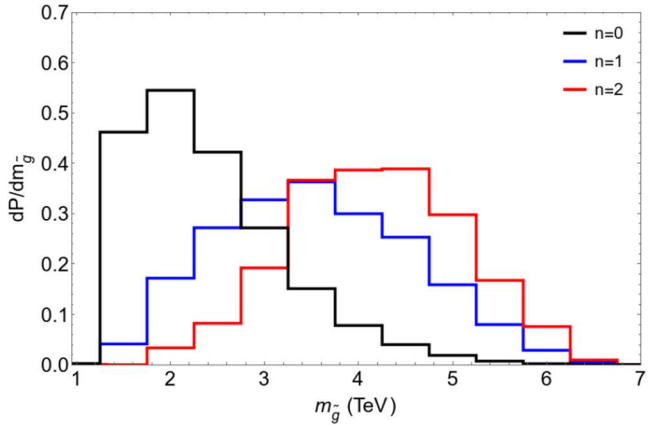

Fig. 19. Distribution in $m_{\tilde{g}}$ after requiring the anthropic selection of $m_{weak} < 350$ GeV.

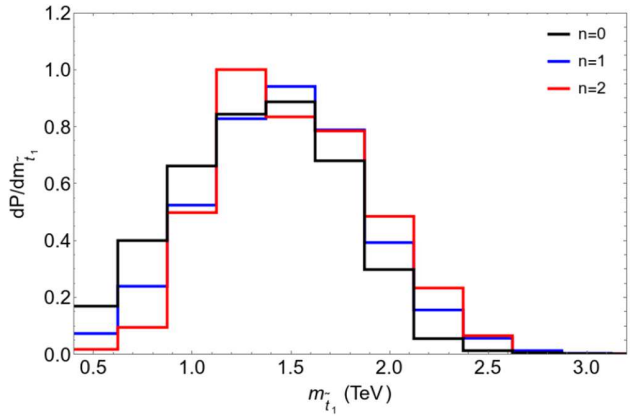

Fig. 20. Distribution in $m_{\tilde{t}_1}$ after requiring the anthropic selection of $m_{weak} < 350$ GeV.

taper off such that hardly any probability is left beyond $m_{\tilde{t}_1} \sim 2.5$ TeV. This upper limit is apparently within reach of high-energy LHC operating with $\sqrt{s} \sim 27$ TeV where the reach in $m_{\tilde{t}_1}$ extends to about 2.5−3 TeV [65].

In Figure 21, we show the distribution $dP/dm_{\tilde{u}_L}$ versus one of the first generation squark masses $m_{\tilde{u}_L}$. Here, it is found for $n = 1,\ 2$ that the distribution peaks around $m_{\tilde{q}} \sim 20{-}25$ TeV– well beyond LHC sensitivity, but in the range to provide at least a partial decoupling solution to the SUSY flavor and CP problems [67]. It would also seem to reflect a rather heavy gravitino mass $m_{3/2} \sim 10{-}30$ TeV in accord with a decoupling solution to the cosmological gravitino problem [159,160]. The $n = 0$ distribution peaks around $m_{\tilde{q}} \sim 8$ TeV and drops steadily to the vicinity of 40 TeV. For much heavier squark masses, then two-loop RGE terms tend to drive the stop sector tachyonic resulting in CCB minima.

4.2 Summary of landscape predictions for Higgs and sparticle masses

From our $n = 1,\ 2$ results which favor a value $m_h \sim 125$ GeV, then we also expect

- $m_{\tilde{g}} \sim 4 \pm 2$ TeV,
- $m_{\tilde{t}_1} \sim 1.5 \pm 0.5$ TeV,

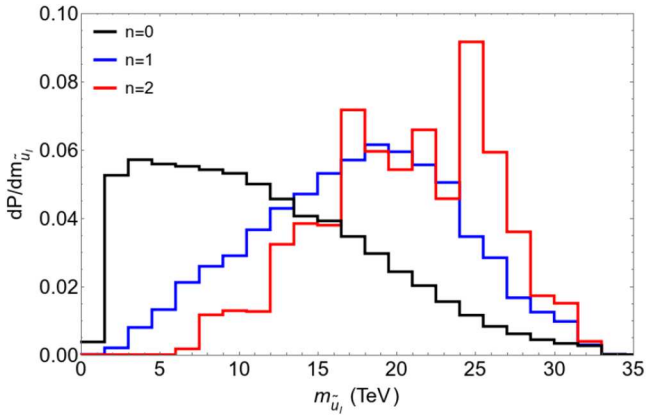

Fig. 21. Distribution in $m_{\tilde{u}_L}$ after requiring the anthropic selection of $m_{weak} < 350$ GeV.

- $m_A \sim 3 \pm 2$ TeV,
- $\tan\beta \sim 13 \pm 7$,
- $m_{\widetilde{\chi}_1,\widetilde{\chi}^0_{1,2}} \sim 200 \pm 100$ GeV and
- $m_{\widetilde{\chi}^0_2} - m_{\widetilde{\chi}^0_1} \sim 7 \pm 3$ GeV with
- $m(\tilde{q}, \tilde{\ell}) \sim 20 \pm 10$ TeV (for first/second generation matter scalars).

These results can provide some guidance as to SUSY searches at future colliders and also a convincing rationale for why SUSY has so far eluded discovery at LHC. They provide a rationale for why SUSY might contain its own decoupling solution to the SUSY flavor and CP problems and the cosmological gravitino and moduli problems. They predict that precision electroweak and Higgs coupling measurements should look very SM-like until the emergence of superpartners at LHC and/or ILC. They also help explain why no WIMP signal has been seen: dark matter may be a higgsino-like-WIMP plus axion admixture with far fewer WIMP targets than one might expect under a WIMP-only dark matter hypothesis [177].

4.3 Related works on SUSY from the landscape

A variety of other issues have been explored in SUSY from the landscape. Below is a brief summary.

- In reference [178], LHC SUSY and WIMP dark matter search constraints confront the string theory landscape. In this case, it is seen that landscape SUSY typically lies well beyond current LHC search limits as presented for various simplified models. In addition, the depleted WIMP abundance from landscape SUSY with a higgsino-like LSP lies below WIMP direct and indirect detection limits- in part because the WIMPs typically make up only 10-20% of the dark matter with the remainder consisting of axions.
- In reference [179], it is examined whether landscape SUSY with the gravity-safe hybrid CCK mixed axion-higgsino-like WIMP dark sector can provide information on the magnitude of the PQ scale f_a. In this case, since SUSY breaking determines f_a, an independent draw on PQ sector soft terms pulls f_a beyond its

sweet spot to yield overproduction of axion dark matter. The overproduction of axions cannot be compensated for by small misalignment angle (as suggested in Refs. [180–182]) since also large f_a causes increased WIMP dark matter due to late-time saxion and axino decays in the early universe. It is concluded that PQ sector soft terms must be correlated with visible sector soft terms and thus lie within the cosmological sweet spot $f_a \sim 10^{11}$ GeV.

- In reference [67], the possibility of a landscape solution to the SUSY flavor and CP problems is investigated. Since the first and second generation soft terms are pulled to common upper bounds, then it is found that a mixed decoupling/degeneracy solution emerges from the landscape with $n \geq 1$ so that the SUSY flavor and CP problems are solved.
- In reference [183], the case of mirage mediation from the landscape is examined wherein there is a landscape draw to large moduli-mediated soft terms as compared to anomaly-mediated soft terms. In this case, for a given value of $m_{3/2}$ (which can be measured in the MM scenario), then probability distributions for the mirage unification scale can be gained: e.g. for $m_{3/2} = 20$ TeV, then one expects gaugino masses to unify around $\mu_{mir} \sim 10^{13-14}$ GeV. The overall Higgs and sparticle mass predictions are similar to NUHM3 except that the gaugino spectrum is compressed.

4.4 Stringy naturalness

For the case of the string theory landscape, in reference [184] Douglas has introduced the concept of *stringy naturalness*:

> **Stringy naturalness:** the value of an observable $\mathcal{O}_2$ is more natural than a value $\mathcal{O}_1$ if more *phenomenologically viable* vacua lead to $\mathcal{O}_2$ than to $\mathcal{O}_1$.

We can compare the usual naturalness measures as shown in Figures 7 and 8 against similar m_0 vs. $m_{1/2}$ planes under stringy naturalness. We generate SUSY soft parameters in accord with equation (20) for various values of $n = 2n_F + n_D - 1 = 1$ and 4. The more stringy natural regions of parameter space are denoted by the higher density of sampled points.

In Figure 22, we show the stringy natural regions for the case of $n = 1$. Of course, no dots lie below the CCB boundary since such minima must be vetoed as they likely lead to an unlivable pocket universe. Beyond the CCB contour, the solutions are in accord with livable vacua. But now the density of points *increases* with increasing m_0 and $m_{1/2}$ (linearly, for $n = 1$), showing that the more stringy natural regions lie at the *highest* m_0 and $m_{1/2}$ values which are consistent with generating a weak scale within the Agrawal bounds. Beyond these bounds, the density of points of course drops to zero since contributions to the weak scale exceed its measured value by a factor 4. There is some fluidity of this latter bound so that values of $\Delta_{EW} \sim 20 - 40$ might also be entertained. The result that stringy naturalness for $n \geq 1$ favors the largest soft terms (subject to m_Z^{PU} not ranging too far from our measured value) stands in stark contrast to conventional naturalness which favors instead the lower values of soft terms. Needless to say, the stringy natural favored region of parameter space is in close accord with LHC results in that LHC find $m_h = 125$ GeV with no sign yet of sparticles.

In Figure 23, we show the same plane under an $n = 4$ draw on soft terms. In this case, the density of dots is clearly highest (corresponding to most stringy natural) at the largest values of m_0 and $m_{1/2}$ as opposed to Figure 8 where the most natural

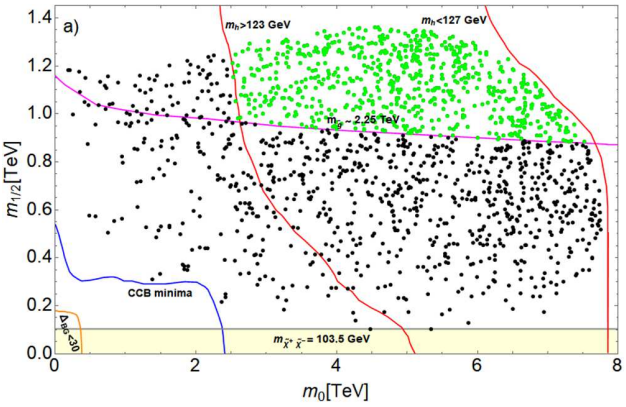

Fig. 22. The m_0 vs. $m_{1/2}$ plane of the NUHM2 model with $A_0 = -1.6m_0$, $\mu = 200$ GeV and $m_A = 2$ TeV and an $n = 1$ draw on soft terms, The higher density of points denotes greater stringy naturalness. The LHC Run 2 limit on $m_{\tilde{g}} > 2.25$ TeV is shown by the magenta curve. The lower yellow band is excluded by LEP2 chargino pair search limits. The green points are LHC-allowed while black are LHC-excluded.

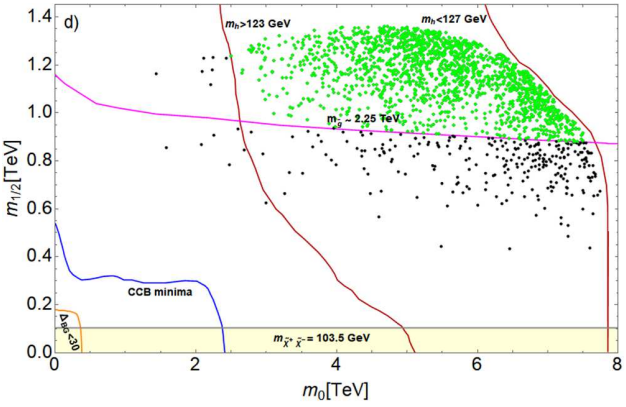

Fig. 23. The m_0 vs. $m_{1/2}$ plane of the NUHM2 model with $A_0 = -1.6m_0$, $\mu = 200$ GeV and $m_A = 2$ TeV and an $n = 4$ draw. The higher density of points denotes greater stringy naturalness. The LHC Run 2 limit on $m_{\tilde{g}} > 2.25$ TeV is shown by the magenta curve. The lower yellow band is excluded by LEP2 chargino pair search limits. The green points are LHC-allowed while black are LHC-excluded.

regions are at low m_0 and $m_{1/2}$. In this sense, under stringy naturalness, a 3 TeV gluino is more natural than a 300 GeV gluino!

5 Comparison of landscape SUSY with other stringy scenarios

5.1 Mini-landscape

A very practical avenue for linking string theory to weak scale physics, known as the mini-landscape, has been investigated at some length [164,165]. The methodology of the mini-landscape is to adopt a toy, but calculable, compactification onto a particular orbifold which is engineered to yield a 4-d low energy theory with many

of the properties of the MSSM. While compactification onto an orbifold may not be ultimately realistic, it is manageable and can yield important lessons [185] as to how the MSSM might arise in more plausible Calabi-Yau compactifications. A key motivation is to aim for a compactification which includes *local* SUSY grand unification [186–188], wherein different regions of the compact space exhibit different gauge symmetries– perhaps including $SU(5)$, or better, $SO(10)$– but where the intersection of these symmetries leads to just the SM gauge group.

Motivated by grand unification, the mini-landscape adopts the $E_8 \times E_8$ gauge structure of the heterotic string since one of the E_8 groups automatically contains as sub-groups the grand unified structures that the SM multiplets and quantum numbers seems to reflect: $E_8 \supset E_6 \supset SO(10) \supset SU(5) \supset G_{\rm SM}$ where $G_{\rm SM} \equiv SU(3)_C \times SU(2)_L \times U(1)_Y$. The other E_8 may contain a hidden sector with $SU(n)$ subgroups which become strongly interacting at some intermediate scale $\Lambda \sim 10^{13}$ GeV leading to gaugino condensation and consequent supergravity breaking [189–192]. Compactification of the heterotic string on a $Z_6 - II$ orbifold [193–196] can lead to low energy theories which include the MSSM, possibly with additional exotic, vector-like matter states (which may decouple).

A detailed exploration of the mini-landscape has been performed a number of years ago. In this picture, the properties of the 4-D low energy theory are essentially determined by the geometry of the 6-D compactified space (orbifold), and by the location (geography) of the various superfields on this space. The gauge group of the 4-D theory is $G_{\rm SM}$ although the symmetry may be enhanced for fields confined to fixed points, or to fixed tori, in the extra dimensions. Examination of the models which lead to MSSM-like structures revealed the following picture [197].

- The first two generations of matter live at orbifold fixed points which exhibit the larger $SO(10)$ gauge symmetry (the twisted sector); thus, first and second generation fermions fill out the 16-dimensional spinor representation of $SO(10)$.

- The Higgs multiplets H_u and H_d live in the untwisted sector and are bulk fields that feel just $G_{\rm SM}$. As such, the Higgs fields come in incomplete GUT multiplets which automatically solves the classic doublet-triplet splitting problem. The gauge superfields also live mainly in the bulk and thus occur in SM representations as well.

- The third generation quark doublet and the top singlet also reside in the bulk, and thus have large overlap with the Higgs fields and correspondingly large Yukawa couplings. The location of other third generation matter fields is model dependent. The small overlap of Higgs and first/second generation fields (which do not extend into the bulk) accounts for their much smaller Yukawa couplings.

- Supergravity breaking may arise from hidden sector gaugino condensation with $m_{3/2} \sim \Lambda^3/m_{\rm P}^2$ with the gaugino condensation scale $\Lambda \sim 10^{13}$ GeV. SUSY breaking effects are felt differently by the various MSSM fields as these are located at different places on the orbifold. Specifically, the Higgs and top squark fields in the untwisted sector feel extended supersymmetry (at tree level) in 4-dimensions, and are thus more protected than the fields on orbifold fixed points which receive protection from just $N = 1$ supersymmetry [198,199]. First/second generation matter scalars are thus expected with masses $\sim m_{3/2}$. Third generation and Higgs soft mass parameters (which enjoy the added protection from extended SUSY) are suppressed by an additional loop factor $\sim 4\pi^2 \sim \log(m_{\rm Pl}/m_{3/2})$. Gaugino masses and trilinear soft terms are expected to be suppressed by the same factor. The suppression of various soft SUSY breaking terms means that (anomaly-mediated) loop contributions [86–89] may

be comparable to modulus- (gravity-) mediated contributions leading to models with mixed moduli-anomaly mediation [99–103] (usually dubbed as *mirage mediation* or MM for short); in the MM scenarios, gaugino masses apparently unify at some intermediate scale

$$\mu_{\rm mir} \sim m_{\rm GUT} e^{-8\pi^2/\alpha}, \tag{25}$$

where α parametrizes the relative amounts of moduli- versus anomaly-mediation.

The spectrum of Higgs bosons and superpartners from the mini-landscape [200] is thus expected to be rather similar to that expected from the full landscape of MSSM theories provided both invoke a *natural* solution to the SUSY μ problem with $\mu \sim 100{-}300$ GeV [183].

5.2 SUSY from IIB string models with moduli stabilization

Upon compactification of string theory to our usual $4-d$ spacetime along with a compact $6-d$ manifold, then one expects a $4d$ effective supergravity theory containing at least the Standard Model fields along with a plethora of moduli fields– massless gravitationally coupled scalar fields which gain mass from fluxes, perturbative corrections to the Kähler potential, or non-perturbative effects. The moduli– grouped as to Hodge number $h^{1,1}$ Kähler moduli (T_i), $h^{1,2}$ complex structure moduli (U_j) and the dilaton S– once stabilized, obtain vevs which determine various parameters of the theory such as gauge and Yukawa couplings etc. Thus, moduli stabilization is one key to making string theory predictive from a top-down approach. Two prominent scenarios for moduli-stabilization in type II-B string theory have emerged.

5.2.1 KKLT

The KKLT [201] scenario makes use of flux compactifications as a route to stabilize the dilaton S and all complex structure moduli U_j at mass scales of order m_{string}. The SM fields are assumed localized on either a $D3$ or $D7$ brane within the compact space. In the original work, a single Kähler modulus T is assumed, and it is assumed to be stabilized by non-perturbative effects such as hidden sector gaugino condensation or the presence of brane instantons leading to a hierarchically smaller mass $m_T \ll m_{string}$. Once all moduli are stabilized, then one is led to a supersymmetric effective theory with an AdS vacuum. The AdS minimum can be uplifted by effects such as adding an anti-$D3$ brane at the tip of a Klebanov-Strassler throat which breaks SUSY and generates a (metastable) de Sitter minimum as required by observation. We note that there has been considerable recent debate on these steps in the context of the string swampland program [202].

The KKLT model is characterized by a mass hierarchy [99–103]

$$m_T \gg m_{3/2} \gg m_{soft}, \tag{26}$$

where the relative strengths are related by a factor $\log(m_P/m_{3/2}) \sim 4\pi^2 \sim 40$. Since one expects $m_{soft} \sim 1$ TeV, then $m_{3/2} \sim 40$ TeV and $m_T \sim 1600$ TeV. With such a hierarchy, then anomaly-mediated contributions to soft terms should be comparable to moduli/gravity-mediated contributions and hence one is led to mirage-mediation soft terms [99–103]. Typically a little hierarchy may arise as well between soft scalar masses and gaugino masses/A-terms. In such a scenario, then one might expect a

mini-split mass hierarchy [203] as shown in Table 6 with $m_{gauginos} \ll m_{scalars}$. In such a case, then one expects large $\Sigma_u^u(\tilde{t}_{1,2})$ contributions to m_{weak} which must be tuned away.

5.2.2 Large volume scenario (LVS)

In the LVS [204], again II-B flux compactification leads to stabilization of the dilaton and complex structure moduli. In order to stabilize Kähler moduli, a compact manifold of the "swiss cheese" variety is selected containing at least two cycles: one large which sets the overall volume of the compact manifold (the overall size of the cheese), and the other(s) quite small corresponding to holes in the cheese. Such a set-up leads to comparable perturbative and non-perturbative contributions to the scalar potential which allow for Kähler moduli stabilization but with an exponentially large manifold volume leading to an effective theory valid up to some intermediate mass scale well below the GUT scale (thus perhaps not consistent with gauge coupling unification or GUTs). The large volume also leads to a disparity in the scales $m_{3/2}$ and m_P. Unlike in KKLT, for LVS, the AdS vacuum already maintains broken SUSY. Like KKLT, uplifting is required to gain a scalar potential of de Sitter type.

The computation of soft terms in the LVS scenario [205] depends on a variety of factors such as whether or not the SM lives on a D3 or a D7 brane and how visible sector moduli are stabilized: non-perturbatively or via D-terms. The various choices lead to LVS models with typically very massive scalars (leading to electroweak unnatural SUSY models). Computation of soft terms using nilpotent goldstino fields and anti-$D3$-branes for uplifting were performed in reference [206]. For LVS with the SM located on a $D3$-brane, then a version of split SUSY is expected to ensue with scalar masses in the 10^3–10^{11} GeV range but with weak scale gauginos. For LVS with the SM localized on a $D7$ brane, then high scale SUSY may be expected with all soft terms/sparticle masses in the 10^3–10^{11} GeV range, as detailed in Table 6.

5.3 M-theory compactified on manifold of G_2 holonomy

In references [207–209],[7] the authors seek to derive general consequences from 11-dimensional M-theory compactified on a manifold of G_2 holonomy. Such a compactification preserves $N = 1$ supersymmetry in the 4-d low energy effective theory, a seemingly necessary phenomenological condition to stabilize the mass of the newly discovered Higgs boson. Then, in the limit of small string coupling and small extra dimensions, the low energy limit of the theory is $N = 1$, $d = 4$ supergravity theory which of necessity includes the MSSM (plus perhaps other exotic matter) along with numerous moduli fields s_i (gravitationally coupled scalar fields which parametrize aspects of the compactification such as the size and shape of extra dimensions) and associated axion fields a_i. The low energy theory is assumed valid just below the Kaluza-Klein scale m_{KK} which is of order $m_{GUT} \sim 2 \times 10^{16}$ GeV. The low energy effective SUGRA theory is then determined by the holomorphic superpotential W, the holomorphic gauge kinetic function(s) f_a (where a labels the gauge group) and the real, non-holomorphic Kähler potential K. The field content of compactified M-theory thus contains the usual matter and gauge superfields, moduli and axions, and possible hidden sector fields. The gravitino gains a mass via hidden sector SUSY breaking so that $m_{3/2} = \sqrt{\sum_i \langle F^i F_i \rangle}/\sqrt{3} m_P$ with m_P the usual 4-d reduced Planck mass. The extra-dimensional gauge symmetry, upon compactification, leads to shift symmetries for the axionic fields which restrict the superpotential to exponentially

[7] For recent reviews, see [210,211].

Table 6. Expected mass range for soft terms/sparticles in a variety of stringy SUSY models along with spectrum nick name.

Soft term	Landscape	Mini-landscape	KKLT-D3/D7	LVS-D3	LVS-D7	G_2MSSM
Gauginos	1–1.5 TeV	$\sim$1 TeV/mirage	$\sim$1 TeV/mirage	$\sim$1 TeV	$\sim 10^{3-11}$ TeV	$\sim$1 TeV
Scalars(1,2)	10–30 TeV	10–30 TeV	$\sim$30 TeV	$\sim 10^{3-11}$ TeV	$\sim 10^{3}$ TeV	$\sim$50 TeV
Scalars(3)	1–5 TeV	1–5 TeV	$\sim$30 TeV	$\sim 10^{3}$ TeV	$\sim 10^{3-11}$ TeV	$\sim$50 TeV
A-terms	$\sim -1.6m_0(3)$	1–5 TeV	$\sim$1 TeV	$\sim$1 TeV	10^{3-11} TeV	$\sim$50 TeV
μ	$0.1-0.3$ TeV	$\sim$0.1$-$1 TeV	$\sim$1 TeV	$\sim$1 TeV	$\sim$10 TeV	$\sim$1 TeV
Nickname	Natural/mirage	Natural/mirage	Mini-split/mirage	Split	High-scale	Mini-split/mirage

suppressed non-perturbative contributions which give rise to suppressed (relative to m_P) scales $W \sim \Lambda^3 \sim e^{-b/\alpha_Q} m_P^3$ plus other suppressed contributions from broken shift symmetries. This results in an exponential hierarchy between $m_{3/2}$ and m_P. With at least two hidden sector gauge groups, then all moduli become stabilized. By including hidden sector matter fields, then the AdS vacuum state is uplifted to de Sitter.

In the G_2MSSM theory, the lightest modulus mass is determined to be of order $m_{3/2}$. To avoid the cosmological modulus problem (moduli decaying too late in the universe and thus upsetting BBN predictions) [212], then $m_{LM} \sim m_{3/2} \sim 30-100$ TeV, where m_{LM} is the mass of the lightest of the moduli. SUSY breaking scalar mass soft terms are then expected to be of order $m_{3/2}$ along with small non-universal contributions. Trilinear soft terms are also of order $m_{3/2}$. Gaugino masses are suppressed from scalar masses by a factor $\log(m_P/m_{3/2}) \sim 30$ and are thus expected of order ∼1 TeV for $m_{3/2} \sim 30$ TeV. The suppressed gaugino masses are thus expected to have comparable moduli- and anomaly-mediated contributions so that the gaugino masses are compressed but with a bino-like LSP. An overabundance of bino-like dark matter is avoided because the light modulus fields alters the relic density computation; its decay injects late-time entropy into the early universe thus diluting all relics, but possibly adding to the LSP abundance: thus, a hallmark feature of this scenario is a non-thermal mixture of axions and WIMPs [213]. The μ parameter is expected to be suppressed by some emergent discrete symmetry but then re-generated at a suppressed level compared to $m_{3/2}$ with $\mu \sim 1$ TeV [214].

Phenomenologically, the above discussion leads to a SUSY spectrum with scalar masses $m_\phi \sim 30-100$ TeV but with a compressed spectrum of gauginos around the TeV scale and higgsinos also ∼1 TeV. Then, the resulting SUSY spectra may be accessible to LHC via gluino pair production followed by $\tilde{g}$ cascade decays [215–225] to mainly 3rd generation quarks plus either a bino or a higgsino LSP [226]. The Higgs mass is expected at $m_h \sim 105-130$ GeV with the region around 125 GeV preferred [227]. In such a set-up, it is hard to understand why the weak scale exists at $m_{weak} \sim 100$ GeV whilst the μ parameter and the $\Sigma_u^u(\tilde{t}_{1,2})$ contributions to m_{weak} are very large and hence require fine-tuning.

6 Implications for SUSY collider searches

6.1 Search for SUSY at LHC

6.1.1 LHC gluino pair searches

In reference [107], the reach of HL-LHC for gluino pair production was evaluated, assuming that $\tilde{g} \to t\tilde{t}_1$ and $\tilde{t}_1 \to b\tilde{\chi}_1^+$ or $t\widetilde{\chi}_{1,2}^0$ and that the decay products of the higgsinos $\tilde{\chi}_1^\pm$ and $\widetilde{\chi}_2^0$ are essentially invisible. For events with $\not{E}_T > 900$ GeV, $n(jets) \geq 4$ and at least two tagged b-jets (plus other cuts detailed in Ref. [107]), it was found that HL-LHC had a 5σ reach for $m_{\tilde{g}}$ of 2.4 (2.6) ((2.8)) TeV for 300 (1000) ((3000)) fb^{-1}, respectively.

In reference [228], the reach of high energy LHC (HE-LHC, LHC with $\sqrt{s} =$ 27 TeV) for both gluinos and top-squarks in the light higgsino scenario was evaluated but with $\sqrt{s} = 33$ TeV. These results were updated for HE-LHC with $\sqrt{s} = 27$ TeV and 15 fb^{-1} of integrated luminosity in reference [65] where more details can be found. A combination of Madgraph, Pythia and Delphes was used to simulate SUSY signal events and SM backgrounds. SM backgrounds included $t\bar{t}$, $t\bar{t}b\bar{b}$, $t\bar{t}t\bar{t}$, $t\bar{t}Z$, $t\bar{t}h$, $b\bar{b}Z$ and single top production. We require at least four hard jets, with two or more tagged as b-jets, no isolated leptons and hard MET and $p_T(jet)$ cuts.

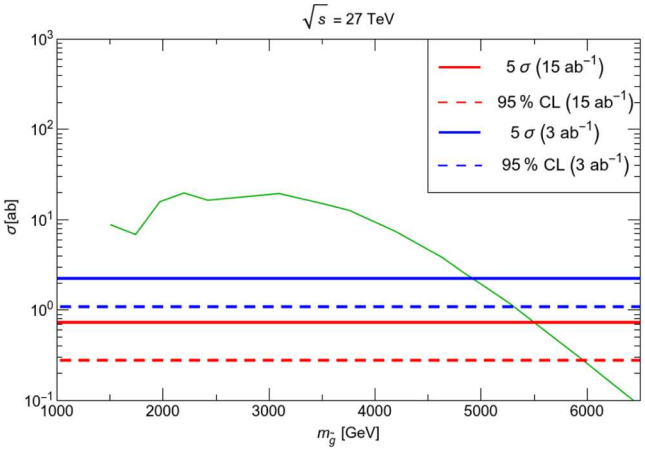

Fig. 24. Plot of gluino pair production cross section vs. $m_{\tilde{g}}$ after cuts at HE-LHC with $\sqrt{s} = 27$ TeV (green curve). We also show the 5σ reach and 95% CL exclusion lines assuming 3 and 15 ab^{-1} of integrated luminosity.

Our results are shown in Figure 24 where we plot the gluino pair production signal versus $m_{\tilde{g}}$ for a natural NUHM2 model line with parameter choice $m_0 = 5m_{1/2}$, $A_0 = -1.6m_0$, $m_A = m_{1/2}$, $\tan\beta = 10$ and $\mu = 150$ GeV with varying $m_{1/2}$. We do not expect the results to be sensitive to this precise choice as long as first generation squarks are much heavier than gluinos. From the figure, we see that the 5σ discovery reach of HE-LHC extends to $m_{\tilde{g}} = 4900$ GeV for 3 ab^{-1} and to $m_{\tilde{g}} = 5500$ GeV for 15 ab^{-1} of integrated luminosity. The corresponding 95% CL exclusion reaches extend to $m_{\tilde{g}} = 5300$ GeV for 3 ab^{-1} and to $m_{\tilde{g}} = 5900$ GeV for 15 ab^{-1} of integrated luminosity. For comparison, the 5σ discovery reach of LHC14 is (2.4) 2.8 TeV for an integrated luminosity of (300) 3000 fb^{-1} [107].

6.1.2 LHC top squark pair searches

In reference [25], the HL-LHC reach for top-squark pair production was evaluated assuming LHC14 with 3000 fb^{-1}. The 95% CL LHC14 reach with 3000 fb^{-1} extends to $m_{\tilde{t}_1} \simeq 1700$ GeV.

In reference [228], the reach of a 33 TeV LHC upgrade for top-squark pair production was investigated. This analysis was repeated using the updated LHC energy upgrade $\sqrt{s} = 27$ TeV. A combination of Madgraph, Pythia and Delphes was again used for SUSY signal and SM background calculations. Top-squark pair production events were generated within a simplified model where $\tilde{t}_1 \to b\widetilde{\chi}_1^+$ at 50%, and $\tilde{t}_1 \to t\widetilde{\chi}_{1,2}^0$ each at 25% branching fraction, which are typical of most SUSY models [229] with light higgsinos. The higgsino-like electroweakino masses are $m_{\widetilde{\chi}_{1,2}^0, \widetilde{\chi}_1^\pm} \simeq 150$ GeV. We required at least two hard b-jets, no isolated leptons and hard $\not{E}_T$ and $p_T(jet)$ cuts: see [65] for details.

Using these background rates for LHC at $\sqrt{s} = 27$ TeV, we compute the 5σ reach and 95% CL exclusion of HE-LHC for 3 and 15 ab^{-1} of integrated luminosity using Poisson statistics. Our results are shown in Figure 25 along with the top-squark pair production cross section after cuts versus $m_{\tilde{t}_1}$. From the figure, we see the 5σ discovery reach of HE-LHC extends to $m_{\tilde{t}_1} = 2800$ GeV for 3 ab^{-1} and to 3160 GeV for 15 ab^{-1}. The 95% CL exclusion limits extend to $m_{\tilde{t}_1} = 3250$ GeV for 3 ab^{-1} and

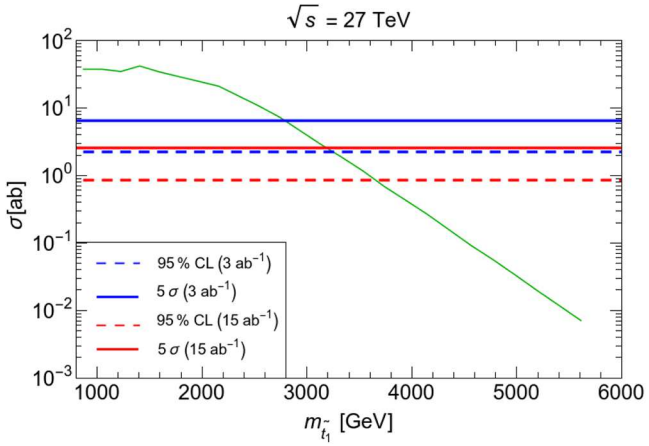

Fig. 25. Plot of top-squark pair production cross section vs. $m_{\tilde{t}_1}$ after cuts at HE-LHC with $\sqrt{s} = 27$ TeV (green curve). We also show the 5σ reach and 95% CL exclusion lines, assuming 3 and 15 ab^{-1} of integrated luminosity.

to $m_{\tilde{t}_1} = 3650$ GeV for 15 ab^{-1}. We checked that S/B exceeds 0.8 whenever we deem the signal to be observable [65].

6.1.3 Combined LHC reach for stops and gluinos

In Figure 26 we exhibit the gluino and top-squark reach values in the $m_{\tilde{t}_1}$ vs. $m_{\tilde{g}}$ plane. We compare the reach of HL- and HE-LHC to values of gluino and stop masses (shown by the dots) in a variety of natural SUSY models defined to have $\Delta_{\rm EW} < 30$ [43,59], including the two- and three-extra parameter non-universal Higgs models [80–85] (nNUHM2 and nNUHM3), natural generalized mirage mediation [104] (nGMM) and natural anomaly-mediation [97] (nAMSB). These models all allow for input of the SUSY μ parameter at values $\mu \sim 100{-}350$ GeV which is a necessary (though not sufficient) condition for naturalness in the MSSM.

The highlight of this figure is that at least one of the gluino or the stop should be discoverable at the HE-LHC. We also see that in natural SUSY models (with the exception of nAMSB), the highest values of $m_{\tilde{g}}$ coincide with the lowest values of $m_{\tilde{t}_1}$ while the highest top squark masses occur at the lowest gluino masses. Thus, a marginal signal in one channel (due to the sparticle mass being near their upper limit) should be accompanied by a robust signal in the other channel. Over most of the parameter range of weak scale natural SUSY there should be a 5σ signal in *both* the top-squark and gluino pair production channels at HE-LHC.

6.1.4 LHC wino pair searches

The wino pair production reaction $pp \to \tilde{\chi}_2^{\pm}\tilde{\chi}_4^0$ can occur at observable rates for SUSY models with light higgsinos. The decays $\tilde{\chi}_2^{\pm} \to W^{\pm}\tilde{\chi}_{1,2}^0$ and $\tilde{\chi}_4^0 \to W^{\pm}\tilde{\chi}_1^{\mp}$ lead to final state dibosons which half the time give a relatively jet-free same-sign diboson signature (SSdB) which has only tiny SM backgrounds [230–232]: see Figure 27.

We have computed the reach of HL-LHC for the SSdB signature in Figure 28 including $t\bar{t}$, WZ, $t\bar{t}W$, $t\bar{t}Z$, $t\bar{t}t\bar{t}$, WWW and $WWjj$ backgrounds. We see that for LHC14 with 3 ab^{-1} of integrated luminosity, the 5σ reach extends to $m(wino) \sim$

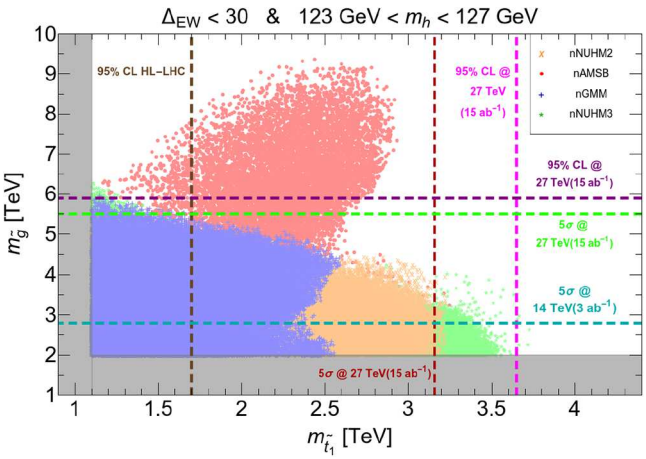

Fig. 26. Plot of points in the $m_{\tilde{t}_1}$ vs. $m_{\tilde{g}}$ plane from a scan over nNUHM2, nNUHM3, nGMM and nAMSB model parameter space. We compare to recent search limits from the ATLAS/CMS experiments and show the projected reach of HL- and HE-LHC. The gray-shaded regions are already excluded by LHC gluino and top-squark searches.

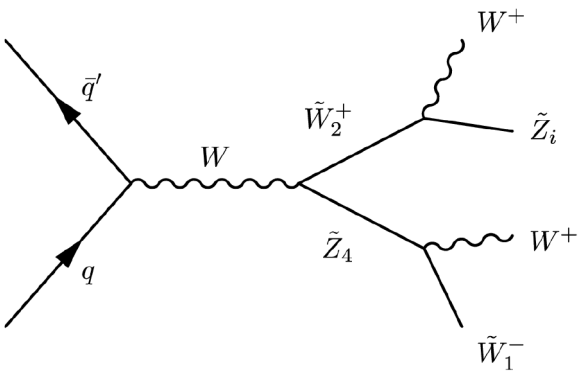

Fig. 27. Feynman diagram for $pp \to \widetilde{\chi}_2^+ \widetilde{\chi}_4^0$ production followed by $\widetilde{\chi}_2^+ \to W^+ \widetilde{\chi}_i^0$ and $\widetilde{\chi}_4^0 \to W^+ \widetilde{\chi}_1^-$ leading to the clean same-sign diboson signature.

860 GeV while the 95% CL exclusion extends to $m(wino) \sim 1080$ GeV. In models with unified gaugino masses, these would correspond to a reach in terms of $m_{\tilde{g}}$ of 2.4 (3) TeV respectively. These values are comparable to what LHC14 can achieve via gluino pair searches with 3 ab^{-1}. The SSdB signature is distinctive for the case of SUSY models with light higgsinos.

While Figure 28 presents the HL-LHC reach for SUSY in the SSdB channel, the corresponding reach of HE-LHC has not yet been computed. The SSdB signal arises via EW production, and the signal rates are expected to rise by a factor of a few by moving from $\sqrt{s} = 14$ TeV to $\sqrt{s} = 27$ TeV. In contrast, some of the QCD backgrounds like $t\bar{t}$ production will rise by much larger factors. Thus, it is not yet clear whether the reach for SUSY in the SSdB channel will be increased by moving from HL-LHC to HE-LHC. We note though that other signals channels from wino decays to higgsinos plus a W, Z and Higgs boson may offer further SUSY detection possibilities.

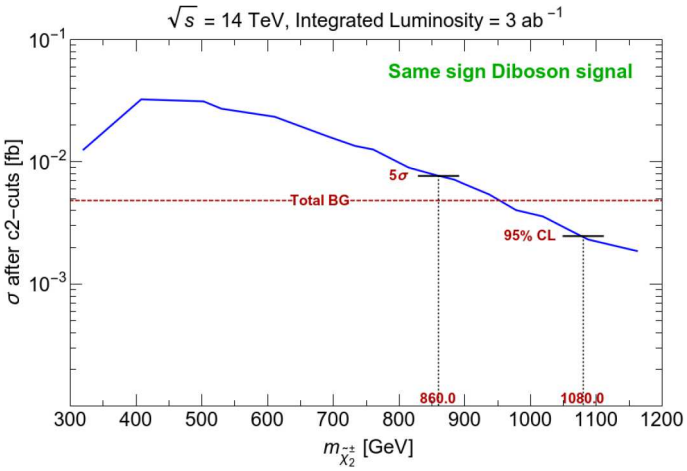

Fig. 28. Cross section for SSdB production (after C2 cuts as delineated in Ref. [232]) versus wino mass at the LHC with $\sqrt{s} = 14$ TeV. We show the 5σ and 95% CL reach assuming a HL-LHC integrated luminosity of 3 ab^{-1}.

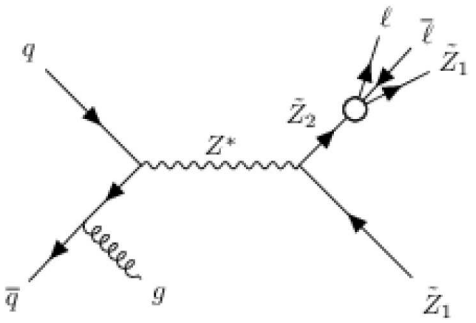

Fig. 29. Feynman diagram for $pp \to \widetilde{\chi}_1^0\widetilde{\chi}_2^0$ production followed by $\widetilde{\chi}_2^0 \to \ell^+\ell^-\widetilde{\chi}_1^0$ plus radiation of a gluon jet from the initial state.

6.1.5 LHC higgsino pair searches

The four higgsino-like charginos $\widetilde{\chi}_1^\pm$ and neutralinos $\widetilde{\chi}_{1,2}^0$ are the only SUSY particles required by naturalness to lie near to the weak scale at $m_{weak} \sim 100$ GeV. In spite of their lightness, they are very challenging to detect at LHC. The lightest neutralino evidently comprises just a portion of dark matter [177], and if produced at LHC via $pp \to \widetilde{\chi}_1^0\widetilde{\chi}_1^0$, $\widetilde{\chi}_1^\pm\widetilde{\chi}_1^\mp$ and $\widetilde{\chi}_1^\pm\widetilde{\chi}_{1,2}^0$ could escape detection. This is because the decay products of $\widetilde{\chi}_2^0$ and $\widetilde{\chi}_1^\pm$ are expected to be very soft, causing the signal to be well below SM processes like WW and $t\bar{t}$ production. The monojet signal arising from initial state QCD radiation $pp \to \widetilde{\chi}_1^0\widetilde{\chi}_1^0 j$, $\widetilde{\chi}_1^\pm\widetilde{\chi}_1^\mp j$ and $\widetilde{\chi}_1^\pm\widetilde{\chi}_{1,2}^0 j$ has been evaluated in [233] and was found to have similar shape distributions to the dominant $pp \to Zj$ background but with background levels about 100 times larger than signal. However, at HE-LHC harder monojet cuts may be possible [234].

A way forward has been proposed via the $pp \to \widetilde{\chi}_1^0\widetilde{\chi}_2^0 j$ channel where $\widetilde{\chi}_2^0 \to \ell^+\ell^-\widetilde{\chi}_1^0$ [64]: a soft OS dilepton pair recoils against a hard initial state jet radiation which serves as a trigger [235,236]: see Figure 29. Recent searches in this

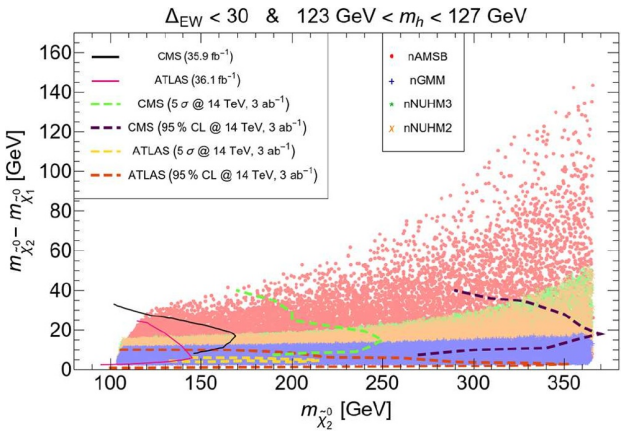

Fig. 30. Plot of points in the $m_{\widetilde{\chi}_2^0}$ vs. $m_{\widetilde{\chi}_2^0} - m_{\widetilde{\chi}_1^0}$ plane from a scan over nNUHM2, nNUHM3, nGMM and nAMSB model parameter space. We compare to recent search limits from the ATLAS/CMS experiments and to future reach contours for HL-LHC (from Ref. [178]).

$\ell^+\ell^- j + MET$ channel have been performed by CMS [237] and by ATLAS [238].[8] Their resultant reach contours are shown as solid black and red contours respectively in the $m_{\widetilde{\chi}_2^0}$ vs. $m_{\widetilde{\chi}_2^0} - m_{\widetilde{\chi}_1^0}$ plane in Figure 30. These searches have indeed probed a portion of promising parameter space since the lighter $m_{\widetilde{\chi}_2^0}$ masses are preferred by naturalness. The ATLAS [240] and CMS experiments [241] have computed some 5σ and 95% CL projected reach contours for HL-LHC with 3 ab^{-1} as the yellow, green, purple and red dashed contours. We see these contours can probe considerably more parameter space although some of natural SUSY parameter space (shown by dots for the same set of models as in Fig. 26) might lie beyond these projected reaches. So far, reach contours for HE-LHC in this search channel have not been computed but it is again anticipated that HE-LHC will not be greatly beneficial here since $pp \to \widetilde{\chi}_1^0\widetilde{\chi}_2^0$ is an electroweak production process so the signal cross section will increase only marginally while QCD background processes like $t\bar{t}$ production will increase substantially.

It is imperative that future search channels try to squeeze their reach to the lowest $m_{\widetilde{\chi}_2^0} - m_{\widetilde{\chi}_1^0}$ mass gaps which are favored to lie in the 3–5 GeV region for string landscape projections [242] of SUSY mass spectra. The ATLAS red-dashed contour appears to go a long way in this regard, though the corresponding 5σ reach is considerably smaller.

6.1.6 Conclusions for natural SUSY at HL- and HE-LHC

We have delineated the reach of the HE-LHC and compared it to the corresponding reach of the HL-LHC for SUSY models with light higgsinos, expected in a variety of natural SUSY models. While the HL-LHC increases the SUSY search range (and may probe the bulk of natural SUSY parameter space at 95% CL in the soft $\ell^+\ell^- j + MET$ channel), it appears that the HE-LHC will definitively probe natural SUSY models with $\Delta_{\rm EW} < 30$ via a 5σ discovery of at least one of the top squark or the gluino (likely even both), possibly also with signals in other channels. Thus, we strongly recommend

[8] The ATLAS collaboration has recently completed an updated study of this reaction using 139 fb^{-1} of data [239].

the construction of an upgraded or new hadron collider with $\sqrt{s} \sim 27{-}100$ TeV in order to fully test natural weak scale SUSY.

6.2 ILC searches

The International Linear e^+e^- Collider, or ILC, is a proposed linear e^+e^- collider to be built in Japan at an initial energy of $\sqrt{s} = 250$ as a Higgs factory. It is expected to be upgradable at later stages to $\sqrt{s} = 500$ and perhaps even 1000 GeV.

6.2.1 Precision measurements at a Higgs factory

The goal of the initial stage of ILC operating at $\sqrt{s} = 250$ GeV is to make detailed precision measurements of the properties of the newly discovered Higgs boson with $m_h \simeq 125$ GeV, mainly via $e^+e^- \to Zh$ production. While greater precision on the Higgs boson mass and spin quantum numbers is always welcome, a more tantalizing avenue towards new physics will be precision measurement of the various Higgs boson decay modes and branching fractions. The presence of new particles, or else virtual effects and modified couplings from physics beyond the Standard Model, are expected to modify the quantities $\kappa_{\tau,b}$, κ_t, $\kappa_{W,Z}$ κ_g and κ_γ which parametrize the ratio of the measured Higgs coupling to SM particles as compared to the coupling as expected from the SM: e.g. $\kappa_b \equiv g_{hb\bar{b}}/g_{hb\bar{b}}(SM)$.

In reference [243], a detailed study of expected values of the κ_i was made for natural SUSY models with $\Delta_{EW} < 30$ and where the models also obeyed LHC8 sparticle and heavy Higgs mass constraints, $m_h = 125 \pm 2$ GeV and bounds from $B \to X_s\gamma$ and $B_s \to \mu^+\mu^-$ decay rates. The presence of two Higgs doublets in the MSSM leads to modified Higgs couplings while the presence of superpartners can modify couplings such as hgg and $h\gamma\gamma$ which occur via loop effects. In that work, it was typically found that the bulk of allowed natural SUSY parameter space leads to very SM-like Higgs couplings since the required rather heavy SUSY particles (except higgsinos) largely decouple and Higgs mixing effects are small. If these results are updated to include LHC Run 2 search results then the expected Higgs couplings will become even more SM-like. Furthermore, in the string landscape picture where soft terms and hence sparticle masses (other than higgsinos) are drawn to large values, then the κ_i values become even more SM-like. While exceptions can occur, for instance if $m_{A,H,H^\pm}$ are in the few hundred GeV range and $\tan\beta$ is small, the general expectation for landscape SUSY is that the ILC Higgs factory precision measurements will see a very SM-like Higgs boson.

6.2.2 Higgsino pair production

While the string landscape is expected to pull soft SUSY breaking terms to large values (subject to not-too-large of contributions to generating a weak scale with $m_{weak} \sim 100$ GeV), the same is not true of the SUSY preserving μ parameter which sets the mass of the lightest higgsino-like electroweakinos. Thus, these latter particles $\widetilde{\chi}^0_{1,2}$ and $\widetilde{\chi}^\pm_1$ offer lucrative targets for an e^+e^- collider operating with $\sqrt{s} > 2m(higgsino) \sim 500{-}600$ GeV [64]. The energy upgrade of the International Linear Collider (ILC) is such a machine [244].

In Figure 31, we show the total production cross sections for a variety of SUSY signal reactions along with dominant SM backgrounds for a typical SUSY mass spectrum from radiative natural SUSY with $\mu \sim 115$ GeV vs. $\sqrt{s}$ of an e^+e^- collider. We see that once the energy threshold $\sqrt{s} = 2\ m(higgsino)$ is passed, then there

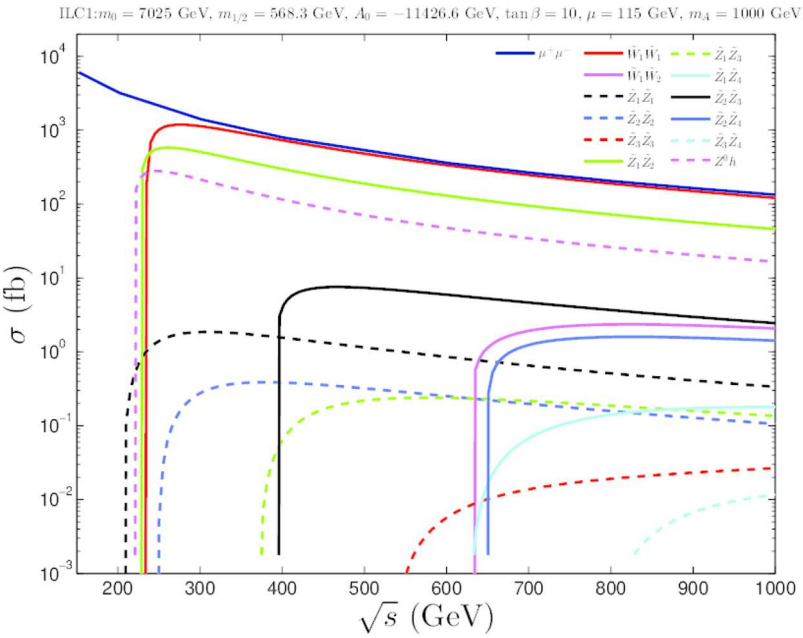

Fig. 31. Sparticle production cross sections vs. $\sqrt{s}$ for unpolarized beams at an e^+e^- collider for the benchmark point labelled as ILC1 in reference [245].

is a rapid rise in the production cross sections for $e^+e^- \to \widetilde{\chi}_1^0\widetilde{\chi}_2^0$ and $\widetilde{\chi}_1^+\widetilde{\chi}_1^-$. Since the mass gaps $m_{\widetilde{\chi}_2^0} - m_{\widetilde{\chi}_1^0}$ and $m_{\widetilde{\chi}_1} - m_{\widetilde{\chi}_1^0}$ are typically 5–15 GeV, then most of the beam energy goes into making the dark matter mass $2m_{\widetilde{\chi}_1^0}$ and the visible decay products of $\widetilde{\chi}_2^0 \to f\bar{f}\widetilde{\chi}_1^0$ and $\widetilde{\chi}_1^\pm \to f\bar{f}'\widetilde{\chi}_1^0$ (the f and f' are SM fermions) are quite soft. Nonetheless, the clean operating environment of an e^+e^- collider will have no trouble picking out such new physics signal events from more energetic SM backgrounds. Detailed analyses are presented in references [245,246]. For these reactions, precision measurements of the difermion invariant mass and energy distributions will allow ILC measurement of $m_{\widetilde{\chi}_1}$, $m_{\widetilde{\chi}_1^0}$ and $m_{\widetilde{\chi}_2^0}$ to percent level precision. This will also allow the SUSY μ parameter to be measured. The higgsino mass splittings are sensitive to the gaugino masses M_1 and M_2 so these can be extracted as well. Extrapolation of the measured gaugino masses to high energy using the RGEs will allow for tests of gaugino mass unification at the GUT scale or at some intermediate mass scale as expected in mirage mediation [246]. Also, extraction of the gaugino vs. higgsino content of the light electroweakinos will allow for insights into the dark matter content of the universe.

6.3 Search for SUSY via lepton flavor violation (LFV)

A complementary way to search for SUSY is via SUSY virtual effects on rare, lepton-flavor violating processes. Such processes include *i*). search for $\mu \to e\gamma$ decay, *ii*). search for $\tau \to \mu\gamma$, *iii*). search for $\mu \to eee$ decay, and search for $\mu \to e$ conversion via $\mu N \to eN$ where N denotes a nuclear target. These various processes have been evaluated for the case of natural SUSY with $\Delta_{EW} < 30$ in reference [247] (for related work, see Ref. [248]). The results depend strongly on the assumed form of the neutrino Yukawa matrix $\mathbf{f}_\nu$. For large mixing similar to the PMNS mixing matrix, then

these processes are typically observable while for small mixing similar to the CKM matrix, then the expected rates are typically below projected sensitivity of upcoming experiment like MEG-II, Belle-II and Mu3e. The results also depend sensitively on whether the SUSY scalars obey a normal mass hierarchy with $m_0(1,2) \ll m_0(3)$ or an inverted scalar mass hierarchy $m_0(3) \ll m_0(1,2)$ as expected from the string landscape and mini-landscape. In the former case, where smuons are lighter, then rates are more promising whilst in the latter case where smuons and muon sneutrinos inhabit the tens-of-TeV regime, then again rates are suppressed.

6.3.1 $(g-2)_\mu$

The above results recall the light/heavy smuon controversy which arises from $(g-2)_\mu$. Current data matched to Standard Model theory predictions find a more than 3σ discrepancy between these values [249]. This discrepancy could be explained by the presence of light smuons with mass $m_{\tilde{\mu}} \sim 0.1{-}1$ TeV (although so far, LHC has seen no sign of these). However, a recent ab initio lattice evaluation of the leading order hadronic vacuum polarization produce theory predictions in close alignment with the measured $(g-2)_\mu$ value [250]. These latter results would be in accord with our expectations for SUSY from the string theory landscape, where one expects smuons in the tens-of-TeV regime, and hence close alignment between SM theory and experiment.

7 Mixed axion plus higgsino-like WIMP dark matter

We have seen that solving the weak scale naturalness problem requires the introduction of weak scale SUSY while solving the QCD naturalness problem requires the PQWW invisible axion [111–117]. The SUSY DFSZ axion naturally solves the SUSY μ problem while yielding a Little Hiararchy $\mu \ll m_{soft}$. A gravity-safe axionic solution to the strong CP problem can emerge from a strong enough anomaly-free discrete R-symmetry $\mathbf{Z}_{24}^R$. In that case, both $U(1)_{PQ}$ and R-parity emerge as accidental, approximate symmetries from the more fundamental discrete R symmetry which in turn may emerge from compactification of 10-d string theory to 4-d. In this very attractive scenario, then dark matter is expected to consist of two particles: a higgsino-like WIMP which is LSP and a SUSY DFSZ axion. Typically, the higgsino-like WIMPs are thermally underproduced with $\Omega_{\tilde{\chi}_1^0}^{TP} h^2 \sim (0.1{-}0.2) \times 0.12$ so that the bulk of dark matter is made of SUSY DFSZ axions. However, now one must include as well the axion superpartners axino $\tilde{a}$ and saxion s into the relic density calculation (along with gravitinos).

7.1 Relic density of mixed axion-higgsino-like WIMP dark matter

To calculate the relic density of mixed axion-WIMP dark matter [251], now one must solve eight coupled Boltzmann equations starting at the temperature of re-heat (at the end of inflation) T_R until the era of entropy conservation [252]. The coupled Boltzmann equations track the energy densities of radiation (SM particles), WIMPs, axinos, saxions, gravitinos and axions. Tracking of coherent oscillation (CO) produced axions and saxions and thermal and decay produced axions and saxions are treated separately. The results of such a calculation for the SUSY DFSZ model [253,254] are shown in Figure 32 from reference [255].

As the PQ-breaking scale f_a increases, then presumably CO-produced axion abundance increases although this can be compensated for by a small axion mis-alignment

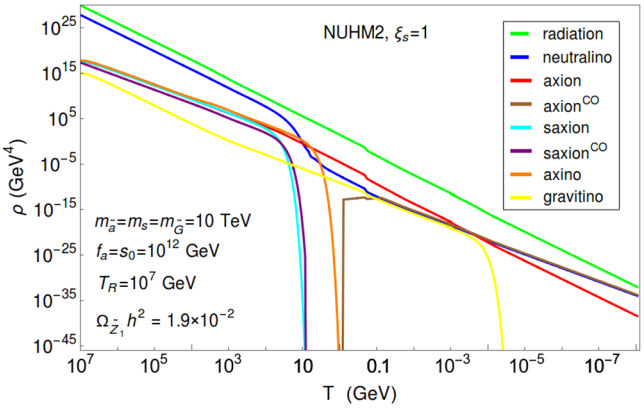

Fig. 32. A plot of various energy densities ρ vs. temperature T starting from $T_R = 10^7$ GeV until the era of entropy conservation from our eight-coupled Boltzmann equation solution to the mixed axion-neutralino relic density in the SUSY DFSZ model for a natural SUSY benchmark point. We take $\xi_s = 1$.

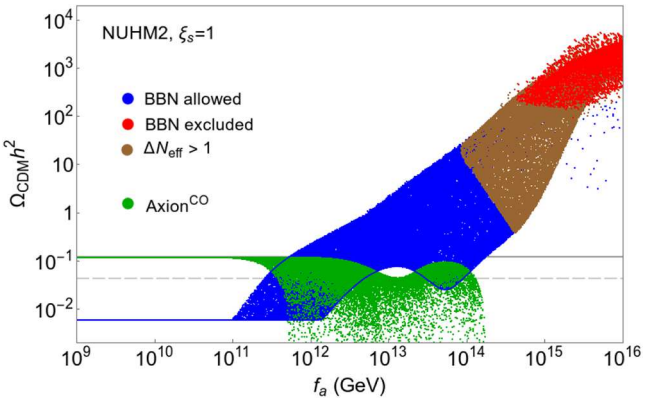

Fig. 33. We plot the relic density of DFSZ axions and higgsino-like WIMPs from a natural SUSY benchmark model using a scan over PQMSSM parameters in the SUSY DFSZ axion model. The dashed line corresponds to 50% of observed Dark Matter relic density.

angle. However, as f_a increases, then axinos and saxions produced in the early universe decay after WIMP freeze-out and give non-thermal contributions to both the WIMP and axion abundance. At too large of f_a values, then mixed WIMP-axion dark matter is overproduced. The result of such a calculation from a scan over PQ parameters is shown in Figure 33. The green dots correspond to the axion relic density while the blue dots correspond to the WIMP relic density. The brown and red dots are excluded by dark radiation constraints ($\Delta N_{eff} > 1$) and BBN constraints, respectively. Values of $f_a \gtrsim 10^{14}$ GeV are completely excluded by overproduction of WIMP dark matter.

7.2 Direct higgsino-like WIMP searches

Even if higgsino-like WIMPs may make up only a fraction of the dark matter, they still may be detected by spin-independent (SI) WIMP direct detection (DD) experiments. In fact, their coupling to Higgs h turns out to be a product of gaugino times

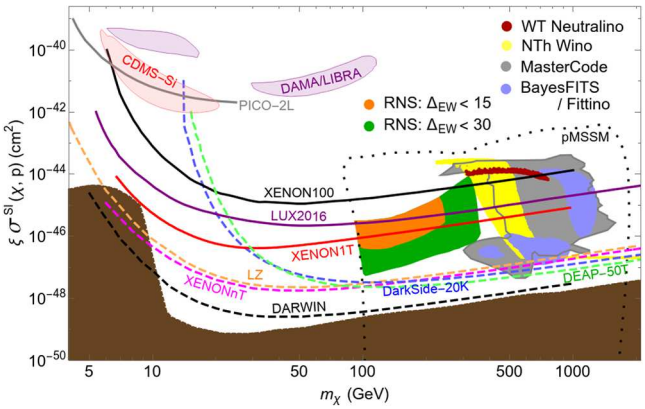

Fig. 34. Plot of rescaled spin-independent WIMP detection rate $\xi\sigma^{SI}(\chi, p)$ versus m_χ from several published results versus current and future reach (dashed) of direct WIMP detection experiments. $\xi = 1$ (i.e. it is assumed WIMPs comprise the totality of DM) for the experimental projections and for all models *except* RNS and pMSSM. The brown region shows the so-called neutrino floor.

higgsino components and is never small since while the WIMPs are mainly higgsino, the naturalness requirement keeps the gaugino component from never going to zero. However, detection rates must be multiplied by the factor $\xi \equiv \Omega_{\widetilde{\chi}_1^0} h^2/0.12$ since now there are fewer WIMPs floating around as they make up only a *portion* of the dark matter. The rates for SI DD are shown in Figure 34 for radiatively-driven natural SUSY (RNS) along with projections from several other SUSY models (updated from Ref. [92]). The predicted theory rates are compared against current WIMP detection limits (solid lines) and future projected limits (dashed lines). While current limits only exclude a portion of natural SUSY parameter space (orange and green regions), the entire natural SUSY parameter space will be explored ultimately by multi-ton noble liquid SI DD experiments. Thus, if no signal is seen by multi-ton SI DD experiments, this basic natural SUSY scenario will be ruled out.

The spin-dependent (SD) DD experiments can also probe natural SUSY parameter space, but must also be multiplied by the fractional relic density parameter ξ. Current limits from IceCube barely touch the natural SUSY parameter space. Future experiments such as Xenon-nton [93], LZ [94] and PICO-500 [95] will probe only a small portion of natural SUSY parameter space. For plots, see reference [92].

Finally, we remark here that the DAMA/LIBRA annual modulation signal and also the gamma-ray excess from the galactic center hint at rather light WIMPs in the 10 GeV regime [96]. Such light WIMPs are difficult to reconcile with natural SUSY where the higgsino-like WIMP is required in the 100-350 GeV regime. If such light WIMPs exist, they should soon be revealed by a bevy of direct (as shown in Fig. 34), indirect and collider search experiments.

7.3 Indirect higgsino-like WIMP searches

It is also possible to search for WIMP-WIMP annihilation into γs and anti-matter at various indirect WIMP detection (IDD) experiments such as Fermi-LAT, HESS, CTA and AMS-II. The theory projections for these searches must all be rescaled by a factor of ξ^2 since now one is looking for WIMP-WIMP annihilation. The ξ^2 factor typically moves the theory projections to regions well below projected sensitivities of the various ID experiments (see Fig. 3 of Ref. [92]).

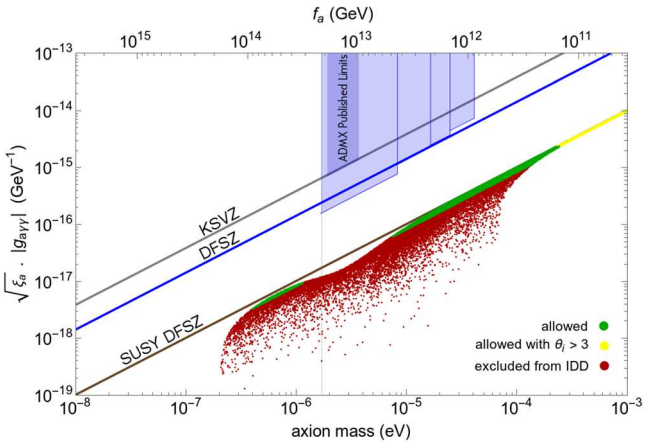

Fig. 35. Axion detection rates at microwave cavity experiments in terms of the axion coupling $g_{a\gamma\gamma}$ vs. m_a. The vertical axis includes a factor $\sqrt{\xi_a}$ where $\xi_a \equiv \Omega_a h^2/0.12$ to account for the depleted abundance of axions. The green points are allowed from natural SUSY while red points are excluded by Fermi-LAT constraints on higgsino-like WIMP annihilation into gamma rays. We also plot lines of SUSY and non-SUSY coupling strengths and current and projected ADMX search regions. The yellow dots are regarded as unnatural since they would require an axion misalignment angle $\theta_i > 3$.

7.4 SUSY DFSZ axion searches

A further possibility for dark matter detection in SUSY models with a DFSZ solution to the strong CP and SUSY μ problems is the detection of relic axions. Microwave cavity experiments are currently making inroads in the m_a vs. $g_{a\gamma\gamma}$ (axion-photon effective coupling) parameter space. The idea here is that relic axions can interact with microwave photons in a super-cooled microwave cavity chamber, and then convert to photons with energy equal to the axion mass. One then searches for bumps in the photon spectra within the cavity.

Usually experiments such as ADMX plot their reach results in the m_a vs. $g_{a\gamma\gamma}$ plane vs. the KSVZ and (non-SUSY) DFSZ axion models. However, in the case of SUSY DFSZ assumed here, the higgsinos also circulate in the $a\gamma\gamma$ anomaly loop. Since the higgsinos necessarily have opposite-sign PQ charge from matter fermions, they will cancel against SM triangle diagrams in the $a\gamma\gamma$ coupling [255]. Along with the anomaly contribution to the $a\gamma\gamma$ coupling, there is a chiral contribution depending on the up- and down-quark masses. In the SUSY DFSZ model, there is a nearly complete cancellation between these two contributions so that the $g_{a\gamma\gamma}$ coupling is highly suppressed. Also, one must multiply by the fractional axion abundance $\xi_a \equiv \Omega_a h^2/0.12$.

The situation is shown in Figure 35 [255]. There, we see that the SUSY DFSZ axion model line is well below current ADMX limits, thus rendering at least for now the SUSY DFSZ axion as *back to invisible*. The green dots show the allowed theory prediction from a scan over NUHM2 model space. Some range of m_a (and correspondingly f_a) is already excluded by WIMP IDD)! This occurs for large enough f_a values that non-thermal production of WIMPs occurs due to late time axino and saxion decays. Then the models have large $\xi(WIMP)$ values and actually are excluded by Fermi-LAT searches.

8 Scenarios for baryogenesis in natural SUSY

One of the main mysteries of particle physics concerns how the matter-antimatter asymmetry arose in the early universe. Starting with Big Bang cosmology, the goal is to explain one number: the baryon-to-photon ratio

$$\eta_B \equiv \frac{n_B}{n_\gamma} \simeq (6.2 \pm 0.5) \times 10^{-10} \quad (95\%\ CL). \tag{27}$$

Production of the baryon asymmetry of the universe or BAU requires mechanisms which satisfy Sakharov's three criteria: 1. baryon number violation, 2. C and CP violation and 3. a departure from thermal equilibrium. In the SM, it is possible to generate the baryon asymmetry via a first order electroweak phase transition, but only if the Higgs mass $m_H \lesssim 50$ GeV, which is obviously excluded. Thus, to produce the measured BAU, new physics is required.

SUSY theories offers a number of different mechanisms for generating the BAU. These include:

- Electroweak baryogenesis: for a strong enough first order EW phase transition, then evidently $m_h \lesssim 113$ GeV with $m_{\tilde{t}_R} \lesssim 115$ GeV is required unless very heavy values of $m_A \gtrsim 10$ TeV are allowed. Such heavy m_A values violate our naturalness conditions where $m_A \simeq m_{H_d}$ and from equation (5) then $m_{H_d} \lesssim \sqrt{m_Z^2/2}\tan\beta \lesssim 4-8$ TeV [256]. Thus, we expect EW baryogenesis in SUSY to be highly implausible.

- Thermal leptogenesis (THL) [257–265]: this mechanism occurs if right-hand-neutrinos can be thermally produced at re-heat temperatures $T_R \gtrsim 1.5 \times 10^9$ GeV, just below upper limits of $T_R \lesssim 10^{10}$ GeV to avoid overproduction of gravitinos, and consequent overproduction of dark matter or disruptions in Big Bang nucleosynthesis (BBN). The thermally produced right-hand neutrinos (RHNs) would decay asymmetrically into leptons versus antileptons and then the lepton asymmetry would wash into the baryon asymmetry via sphaleron effects.

- Non-thermal leptogenesis (NTHL) [266–271]: Here it is assumed the production of RHNs takes place via inflaton decay in the early universe. In this case, re-heat temperatures of just $T_R \gtrsim 10^6$ GeV are required.

- Leptogenesis from oscillating sneutrino decay (OSL) [272]: In this case, the heavy *sneutrinos* are produced via coherent oscillations and their decays generate the lepton asymmetry which is again washed into the baryon asymmetry via sphalerons.

- Affleck-Dine leptogenesis (ADL) [273,274]: Usual Affleck-Dine baryogenesis [275] is afflicted by various problems such as Q-ball production. However, Affleck-Dine *leptogenesis* [273,274] is perfectly viable. ADL uses the LH_u flat direction in the SUSY scalar potential to generate a condensate carrying non-zero lepton number. The condensate oscillates and then decays asymmetrically to generate the lepton asymmetry which is again converted to the baryon asymmetry via the sphaleron.

For natural SUSY models with a μ parameter generated via the SUSY DFSZ axion sector, then the baryon asymmetry relies on the SUSY soft breaking scale $m_{3/2}$, the re-heat temperature T_R and the PQ sector parameters such as f_a, the axino mass $m_{\tilde{a}}$, the saxion mass m_s and ξ_s which governs whether the saxion decays to axinos and

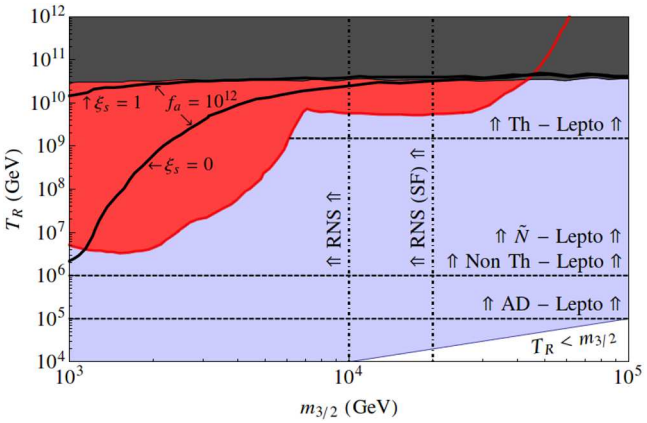

Fig. 36. Plot of allowed regions in T_R vs. $m_{3/2}$ plane in the SUSY DFSZ axion model for $f_a = 10^{11}$ and 10^{12} GeV for $\xi_s = 0$. For $f_a = 10^{11}$, $T_R > 10^{11}$ is forbidden to avoid PQ symmetry restoration. We take $m_s = m_{\tilde{a}} \equiv m_{3/2}$ (from Refs. [276,277]).

axions ($\xi_s = 1$) or not ($\xi_s = 0$). The viable regions for the different mechanisms are shown in Figure 36 [276,277] for $f_a = 10^{11}$ GeV or 10^{12} GeV and for $\xi_s = 0$ or 1. The upper black-shaded region is excluded by overproduction of WIMPs from gravitino decay. The red-shaded region is excluded by disruption of BBN. The various allowed regions are labeled as are the regions that accommodate radiatively-driven natural SUSY (RNS) with universal or split families (SF). From the plot, it can be seen that only a small region of THL is allowed, but in contrast large regions of parameter space are allowed for successful baryogenesis via NTHL, ADL or OSL. Finally, for the lower-right region with $T_R < m_{3/2}$, then none of the examined mechanisms would apply and perhaps some sort of alternative baryogenesis mechanism would be required (see e.g. Ref. [278] for a WIMP baryogenesis alternative).

9 Conclusions

In this midi-review, we have sought to outline the status of weak scale supersymmetry [6] as it stands after LHC13 Run 2 with 139 fb^{-1} of data and after first results from ton-scale noble liquid direct WIMP searches. At first sight, the lack of WIMP signals along with the seemingly severe sparticle mass limits from LHC, as compared to early naturalness-derived upper bounds on sparticle masses, has led much of the HEP community to a rather pessimistic attitude towards the vitality of the weak scale SUSY paradigm.

However, as noted in the Introduction, the latest experimental limits are usually compared against an early cartoonish picture as to how weak scale SUSY would manifest itself. Several important developments in the 21st century have required a change in the WSS paradigm. These include:

- a clarification of the notion of weak scale naturalness in SUSY (a summary Tab. 7 is provided which presents each naturalness measure, its definition, motivation and some principle consequences),

- the influence of including a (axionic) solution to the strong CP problem into the SUSY paradigm,

Table 7. Summary of naturalness measures along with definition, motivation and some principle consequences. The superscripts *PU* stands for *pocket universe* while *OU* stands for *our universe*. Tabular formatting precludes us from adding a fifth column on *limitations* for each measure, so we include this information here. Δ_{BG}: parameter, scale and model dependent; Δ_{HS}: oversimplified, breaks measure into *dependent* terms; Δ_{EW}: model-independent within MSSM, but may require additional terms for extended models; *stringy*: depends on string multiverse/landscape paradigm.

Measure	Definition	Motivation	Consequences
Δ_{BG}	$max_i\vert\frac{p_i}{m_Z^2}\frac{\partial m_Z^2}{\partial p_i}\vert$	Measure fine-tuning of effective theory parameters p_i to obtain measured m_Z	Favors soft terms at or around m_{weak}
Δ_{HS}	$\delta m_{H_u}^2/m_h^2$	Require small change in running contribution To m_h	$m_{\tilde{t}_{1,2}}, m_{\tilde{b}_1} \lesssim 500$ GeV small A_t
Δ_{EW}	$\vert largest\ cont.\ to\ m_Z^2/2\vert/\ m_Z^2/2$	Parameter indep. measure based on practical Naturalness	Require $\mu \sim 100-300$ GeV and highly mixed stops $m_{\tilde{t}_1} \lesssim 3$ TeV; allow radiatively-driven naturalness
stringy	Largest contribution to $m_{weak}^{PU} < (2-5)m_{weak}^{OU}$ with power-law draw to large soft terms	String landscape	Pull sparticles beyond LHC limits with $m_h \to 125$ GeV; radiatively-driven naturalness

– the emergence of discrete R-symmetries and their role in the SUSY μ problem, suppression of proton-decay, and as a source for the emergence of the accidental, approximate R-parity and gravity-safe global PQ symmetry,

– the emergence of the string theory landscape and its role in solving the cosmological constant problem and setting the scale for SUSY breaking and electroweak symmetry breaking, its role in solving the SUSY flavor and CP problems, and the implications of stringy naturalness.

We presented here a midi-review of recent work that seeks to update the WSS paradigm by addressing these concerns. The emergent picture of weak scale BSM physics includes the following.

– Retention of WSS to stabilize the Higgs mass and retain the successful agreement between virtual effects within the MSSM and data including 1. measured strengths of weak scale gauge couplings and gauge coupling unification within the MSSM, 2. the measured value of m_t and its role in seeding a radiative breakdown of EW symmetry, 3. the measured value of $m_h \simeq 125$ GeV and its consistency with MSSM predictions including highly-mixed, TeV-scale top squarks and 4. precision EW measurements of m_W vs. m_t which favor soft terms in the multi-TeV range.

– Requirement of *practical naturalness* wherein weak scale SUSY contributions to the magnitude of the weak scale are comparable to the weak scale. This requires the SUSY-conserving μ parameter not too far from $m_{weak} \sim m_{W,Z,h} \sim 100$ GeV while soft SUSY breaking terms, which enter the weak scale via loop-supressed terms, can range into the TeV or even tens of TeV regime. The higgsinos are then the lightest superpartners and one expects a mainly higgsino-like LSP. This has major consequences for both collider and dark matter signatures.

– Inclusion of a (gravity-safe) PQ sector to solve the strong CP problem. This may involve a Kim-Nilles solution to the SUSY μ problem with a Little Hierarchy $\mu \ll m_{soft}$ which is still natural. The gravity-safe $U(1)_{PQ}$ and R-parity could both emerge from a more fundamental anomaly-free discrete R-symmetry such as $\mathbf{Z}_{24}^R$ which in turn is interpreted as the discrete remnant of compactification of 10-d Lorentz symmetry down to 4-dimensions. The discrete R symmetry also plays a role in suppressing dangerous dimension 5 proton decay operators.

– The inclusion of the string landscape allows for Weinberg's anthropic solution to the cosmological constant problem. Under rather general stringy considerations, the landscape should also statistically favor soft SUSY breaking terms as large as possible subject to the condition that contributions to the weak scale are comparable to the weak scale (within a factor 2–5 [53,54]). This leads to a statistical pull on $m_h \to 125$ GeV whilst pulling most sparticle masses to beyond LHC limits [242]. In fact, under stringy naturalness, a 3 TeV gluino is more natural than a 300 GeV gluino [56]! The exceptions to TeV-level sparticle masses are the light higgsinos whose mass term is SUSY conserving and arises from whatever mechanism solves the SUSY μ problem (such as the gravity-safe hybrid CCK models based on $\mathbf{Z}_{24}^R$ symmetry).

While the emergent WSS paradigm includes solutions to a host of problems which were typically previously neglected, it also leads to new collider signatures. While an LHC upgrade to at least $\sqrt{s} \sim 27$ TeV may be needed to access gluinos and top squarks, a corroborative signature emerges in SUSY with light higgsinos; the ultimate appearance of same-sign W-boson pairs arising from wino pair production followed by decay to higgsinos. However, the most lucrative signature for natural landscape

SUSY appears to be the soft OS/SF dilepton plus jet signature arising from direct higgsino pair production [64]. HL-LHC may be able to explore a sizable chunk of natural SUSY parameter space via this novel signature, which should slowly emerge as more and more integrated luminosity accrues. The OS/SF dilepton invariant mass is bounded by the inter-higgsino mass gap $m(\ell^+\ell^-) < m_{\widetilde{\chi}_2^0} - m_{\widetilde{\chi}_1^0} \sim 5{-}10$ GeV which makes for challenging searches for very soft dileptons at ATLAS and CMS.

In the updated WSS paradigm, we can also understand why WIMPs have not yet been detected. We now expect mixed axion with higgsino-like-WIMP dark matter where the WIMPs typically make up only 10-20% of the dark matter whilst axions make up the remainder. Multi-ton noble liquid dark matter detectors will be needed to probe the entire predicted parameter space. Indirect WIMP detection seems rather unlikely in the near future since detection rates are suppressed by the square of the fractional WIMP abundance. Axion detection via microwave cavity experiments also seem unlikely in the near-term since the presence of higgsinos in the $g_{a\gamma\gamma}$ coupling leads to cancellations and consequently suppressed axion couplings to photons [255].

Overall, the updated weak scale SUSY paradigm– as manifested in natural landscape SUSY– predicts that LHC at this time should see a Higgs boson with $m_h \sim 125$ GeV but as yet no signals from sparticles. Indeed, updated experimental facilities– a higher energy LHC with $\sqrt{s} \sim 27{-}100$ TeV and/or a $\sqrt{s} > 2m(higgsino)$ linear collider may be needed for SUSY discovery. As well, we may have to await a full exploration of relic WIMP parameter space by multi-ton noble liquid detectors for verification or falsification of the presence of WIMPs from weak scale SUSY.

We thank our many collaborators for their dedicated contributions to this midi-review. We especially thank H. Serce for updating Figure 34, and for his many contributions to this work. This material is based upon work supported by the U.S. Department of Energy, Office of Science, Office of High Energy Physics under Award Number DE-SC-0009956.

References

1. G. Aad et al. [ATLAS Collaboration], Phys. Lett. B **716**, 1 (2012)
2. S. Chatrchyan et al. [CMS Collaboration], Phys. Lett. B **716**, 30 (2012)
3. L. Susskind, Phys. Rev. D **20**, 2619 (1979)
4. E. Witten, Nucl. Phys. B **188**, 513 (1981)
5. R.K. Kaul, Phys. Lett. B **109**, 19 (1982)
6. H. Baer, X. Tata, *Weak scale supersymmetry: From superfields to scattering events* (Cambridge University Press, Cambridge, UK, 2006)
7. S. Dimopoulos, S. Raby, F. Wilczek, Phys. Rev. D **24**, 1681 (1981)
8. K. Inoue, A. Kakuto, H. Komatsu, S. Takeshita, Prog. Theor. Phys. **68**, 927 (1982) [Erratum: Prog. Theor. Phys. **70**, 330 (1983)]
9. L. Alvarez-Gaume, J. Polchinski, M.B. Wise, Nucl. Phys. B **221**, 495 (1983)
10. K. Inoue, A. Kakuto, H. Komatsu, S. Takeshita, Prog. Theor. Phys. **71**, 413 (1984)
11. L.E. Ibañez, G.G. Ross, Phys. Lett. B **110**, 215 (1982)
12. K. Inoue et al. Prog. Theor. Phys. **68**, 927 (1982)
13. K. Inoue et al. Prog. Theor. Phys. **71**, 413 (1984)
14. L. Ibañez, Phys. Lett. B **118**, 73 (1982)
15. H.P. Nilles, M. Srednicki, D. Wyler, Phys. Lett. B **120**, 346 (1983)
16. J. Ellis, J. Hagelin, D. Nanopoulos, M. Tamvakis, Phys. Lett. B **125**, 275 (1983)
17. L. Alvarez-Gaumé. J. Polchinski, M. Wise, Nucl. Phys. B **221**, 495 (1983)
18. B.A. Ovrut, S. Raby, Phys. Lett. B **130**, 277 (1983)

19. For a review, see L.E. Ibanez, G.G. Ross, C. R. Physique **8**, 1013 (2007)
20. M. Carena, H.E. Haber, Prog. Part. Nucl. Phys. **50**, 63 (2003)
21. P. Draper, H. Rzehak, Phys. Rep. **619**, 1 (2016)
22. S. Heinemeyer, W. Hollik, D. Stockinger, A.M. Weber, G. Weiglein, JHEP **0608**, 052 (2006)
23. M. Aaboud et al. [ATLAS Collaboration], Phys. Rev. D **97**, 112001 (2018)
24. T.A. Vami [ATLAS and CMS Collaborations], PoS LHCP **2019**, 168 (2019)
25. The ATLAS collaboration [ATLAS Collaboration], ATLAS-CONF-2019-017, 2019
26. A.M. Sirunyan et al. [CMS Collaboration], arXiv:1912.08887 [hep-ex]
27. A. Canepa, Rev. Phys. **4**, 100033 (2019)
28. E. Aprile et al. [XENON Collaboration], Phys. Rev. Lett. **121**, 111302 (2018)
29. J.L. Feng, K.T. Matchev, T. Moroi, Phys. Rev. D **61**, 075005 (2000)
30. J.L. Feng, K.T. Matchev, T. Moroi, arXiv:hep-ph/0003138
31. J.L. Feng, D. Sanford, Phys. Rev. D **86**, 055015 (2012)
32. N. Arkani-Hamed, A. Delgado, G.F. Giudice, Nucl. Phys. B **741**, 108 (2006)
33. H. Baer, A. Mustafayev, E.K. Park, X. Tata, JCAP **0701**, 017 (2007)
34. H. Baer, A. Mustafayev, E.K. Park, X. Tata, JHEP **0805**, 058 (2008)
35. R. Barbieri, G.F. Giudice, Nucl. Phys. B **306**, 63 (1988)
36. For a review, see e.g. R. Arnowitt, P. Nath, in *Perspectives on Supersymmetry II*, edited by G.L. Kane (World Scientific, Singapore, 2010), pp. 222–243 and references therein
37. V.D. Barger, M.S. Berger, P. Ohmann, Phys. Rev. D **47**, 1093 (1993)
38. V.D. Barger, M.S. Berger, P. Ohmann, Phys. Rev. D **49**, 4908 (1994)
39. G.L. Kane, C.F. Kolda, L. Roszkowski, J.D. Wells, Phys. Rev. D **49**, 6173 (1994)
40. S. Cassel, D.M. Ghilencea, G.G. Ross, Phys. Lett. B **687**, 214 (2010)
41. M. Papucci, J.T. Ruderman, A. Weiler, JHEP **1209**, 035 (2012)
42. C. Brust, A. Katz, S. Lawrence, R. Sundrum, JHEP **1203**, 103 (2012)
43. H. Baer, V. Barger, P. Huang, A. Mustafayev, X. Tata, Phys. Rev. Lett. **109**, 161802 (2012).
44. K.J. Bae, H. Baer, V. Barger, D. Sengupta, Phys. Rev. D **99**, 115027 (2019)
45. H.M. Lee, S. Raby, M. Ratz, G.G. Ross, R. Schieren, K. Schmidt-Hoberg, P.K.S. Vaudrevange, Nucl. Phys. B **850**, 1 (2011)
46. For a review, see M.C. Chen, M. Fallbacher, M. Ratz, Mod. Phys. Lett. A **27**, 1230044 (2012)
47. H.P. Nilles, PoS (CORFU2016) 017, in *Proceedings of the Corfu Summer Institute 2016 "School and Workshops on Elementary Particle Physics and Gravity"*, 31 August - 23 September, 2016, Corfu, Greece
48. R. Bousso, J. Polchinski, JHEP **2000**, JHEP06 (2000)
49. L. Susskind, in *Universe or multiverse?* edited by B. Carr (Cambridge University Press, 2007), pp. 247–266
50. R. Bousso, J. Polchinski, Sci. Am. **291**, 60 (2004)
51. S. Weinberg, Phys. Rev. Lett. **59**, 2607 (1987)
52. M.R. Douglas, arXiv:hep-th/0405279
53. V. Agrawal, S.M. Barr, J.F. Donoghue, D. Seckel, Phys. Rev. D **57**, 5480 (1998)
54. V. Agrawal, S.M. Barr, J.F. Donoghue, D. Seckel, Phys. Rev. Lett. **80**, 1822 (1998)
55. H. Baer, V. Barger, H. Serce, K. Sinha, JHEP **1803**, 002 (2018)
56. H. Baer, V. Barger, S. Salam, Phys. Rev. Research. **1**, 023001 (2019)
57. M. van Beekveld, W. Beenakker, S. Caron, R. Peeters, R. Ruiz de Austri, Phys. Rev. D **96**, 035015 (2017)
58. M. van Beekveld, S. Caron, R. Ruiz de Austri, JHEP **2001**, 147 (2020)
59. H. Baer, V. Barger, P. Huang, D. Mickelson, A. Mustafayev, X. Tata, Phys. Rev. D **87**, 115028 (2013)
60. H. Baer, V. Barger, M. Savoy, Phys. Rev. D **93**, 035016 (2016)
61. K.L. Chan, U. Chattopadhyay, P. Nath, Phys. Rev. D **58**, 096004 (1998)
62. S. Akula, M. Liu, P. Nath, G. Peim, Phys. Lett. B **709**, 192 (2012)
63. M. Liu, P. Nath, Phys. Rev. D **87**, 095012 (2013)
64. H. Baer, V. Barger, P. Huang, JHEP **1111**, 031 (2011)

65. H. Baer, V. Barger, J.S. Gainer, D. Sengupta, H. Serce, X. Tata, Phys. Rev. D **98**, 075010 (2018)
66. H. Baer, V. Barger, M. Padeffke-Kirkland, X. Tata, Phys. Rev. D **89**, 037701 (2014)
67. H. Baer, V. Barger, D. Sengupta, Phys. Rev. Res. **1**, 033179 (2019)
68. H. Baer, V. Barger, A. Mustafayev, Phys. Rev. D **85**, 075010 (2012)
69. H. Baer, V. Barger, D. Mickelson, Phys. Rev. D **88**, 095013 (2013)
70. H. Baer, V. Barger, D. Mickelson, M. Padeffke-Kirkland, Phys. Rev. D **89**, 115019 (2014)
71. H. Baer, V. Barger, M. Savoy, Phys. Scr. **90**, 068003 (2015)
72. J.R. Ellis, K. Enqvist, D.V. Nanopoulos, F. Zwirner, Mod. Phys. Lett. A **1**, 57 (1986)
73. L.E. Ibanez, C. Lopez, C. Munoz, Nucl. Phys. B **256**, 218 (1985)
74. A. Lleyda, C. Munoz, Phys. Lett. B **317**, 82 (1993)
75. H. Abe, T. Kobayashi, Y. Omura, Phys. Rev. D **76**, 015002 (2007)
76. S.P. Martin, Phys. Rev. D **75**, 115005 (2007)
77. For a recent review, see e.g. J.L. Feng, Ann. Rev. Nucl. Part. Sci. **63**, 351 (2013)
78. A. Mustafayev, X. Tata, Indian J. Phys. **88**, 991 (2014)
79. H. Baer, V. Barger, P. Huang, D. Mickelson, M. Padeffke-Kirkland, X. Tata, Phys. Rev. D **91**, 075005 (2015)
80. D. Matalliotakis, H.P. Nilles, Nucl. Phys. B **435**, 115 (1995)
81. M. Olechowski, S. Pokorski, Phys. Lett. B **344**, 201 (1995)
82. P. Nath, R.L. Arnowitt, Phys. Rev. D **56**, 2820 (1997)
83. J. Ellis, K. Olive, Y. Santoso, Phys. Lett. B **539**, 107 (2002)
84. J. Ellis, T. Falk, K. Olive, Y. Santoso, Nucl. Phys. B **652**, 259 (2003)
85. H. Baer, A. Mustafayev, S. Profumo, A. Belyaev, X. Tata, JHEP **0507**, 065 (2005)
86. L. Randall, R. Sundrum, Nucl. Phys. B **557**, 79 (1999)
87. G.F. Giudice, M. Luty, H. Murayama, R. Rattazzi, JHEP **9812**, 027 (1998)
88. J. Bagger, T. Moroi, E. Poppitz, JHEP **0004**, 009 (2000)
89. P. Binetruy, M.K. Gaillard, B. Nelson, Nucl. Phys. B **604**, 32 (2001)
90. T. Cohen, M. Lisanti, A. Pierce, T.R. Slatyer, JCAP **1310**, 061 (2013)
91. J. Fan, M. Reece, JHEP **1310**, 124 (2013)
92. H. Baer, V. Barger, H. Serce, Phys. Rev. D **94**, 115019 (2016)
93. E. Aprile et al. [XENON], JCAP **04**, 027 (2016)
94. D. Akerib et al. [LZ], arXiv:1509.02910 [physics.ins-det]
95. C. Amole et al. [PICO], EPJ Web Conf. **95**, 04020 (2015)
96. G.B. Gelmini, Rept. Prog. Phys. **80**, 082201 (2017)
97. H. Baer, V. Barger, D. Sengupta, Phys. Rev. D **98**, 015039 (2018)
98. K.J. Bae, H. Baer, A. Lessa, H. Serce, Front. Phys. **3**, 49 (2015)
99. K. Choi, A. Falkowski, H.P. Nilles, M. Olechowski, S. Pokorski, JHEP **0411**, 076 (2004)
100. K. Choi, A. Falkowski, H.P. Nilles, M. Olechowski, Nucl. Phys. B **718**, 113 (2005)
101. J.P. Conlon, F. Quevedo, K. Suruliz, JHEP **0508**, 007 (2005)
102. A. Pierce, J. Thaler, JHEP **0609**, 017 (2006)
103. B.L. Kaufman, B.D. Nelson, M.K. Gaillard, Phys. Rev. D **88**, 025003 (2013)
104. H. Baer, V. Barger, H. Serce, X. Tata, Phys. Rev. D **94**, 115017 (2016)
105. H. Baer, F. Paige, S. Protopopescu, X. Tata, arXiv:hep-ph/0312045
106. S. Dimopoulos, G.F. Giudice, **357**, 573 (1995)
107. H. Baer, V. Barger, J.S. Gainer, P. Huang, M. Savoy, D. Sengupta, X. Tata, Eur. Phys. J. C **77**, 499 (2017)
108. S. Weinberg, Phys. Rev. D **11**, 3583 (1975)
109. G. 't Hooft, Phys. Rev. Lett. **37**, 8 (1976)
110. R.D. Peccei, AIP Conf. Proc. **1274**, 7 (2010)
111. R.D. Peccei, H.R. Quinn, Phys. Rev. Lett. **38**, 1440 (1977)
112. S. Weinberg, Phys. Rev. Lett. **40**, 223 (1978)
113. F. Wilczek, Phys. Rev. Lett. **40**, 279 (1978)
114. J.E. Kim, Phys. Rev. Lett. **43**, 103 (1979)
115. M.A. Shifman, A. Vainstein, V.I. Zakharov, Nucl. Phys. B **166**, 493 (1980)
116. M. Dine, W. Fischler, M. Srednicki, Phys. Lett. B **104**, 199 (1981)

117. A.P. Zhitnitskii, Sov. J. Phys. **31**, 260 (1980)
118. L.F. Abbott, P. Sikivie, Phys. Lett. B **120**, 133 (1983)
119. J. Preskill, M. Wise, F. Wilczek, Phys. Lett. B **120**, 127 (1983)
120. M. Dine, W. Fischler, Phys. Lett. B **120**, 137 (1983)
121. M. Turner, Phys. Rev. D **33**, 889 (1986)
122. J.E. Kim, H.P. Nilles, Phys. Lett. B **138**, 150 (1984)
123. E.J. Chun, Phys. Rev. D **84**, 043509 (2011)
124. K.J. Bae, E.J. Chun, S.H. Im, JCAP **1203**, 013 (2012)
125. B. Carter, The general theory of the mechanical, electromagnetic and thermodynamic properties of black holes, in Conference proceedings *General Relativity: An Einstein centenary survey* (1979), pp. 294–369
126. S.B. Giddings, A. Strominger, Nucl. Phys. B **306**, 890 (1988)
127. G. Gilbert, Nucl. Phys. B **328**, 159 (1989)
128. R. Kallosh, A.D. Linde, D.A. Linde, L. Susskind, Phys. Rev. D **52**, 912 (1995)
129. B.A. Dobrescu, Phys. Rev. D **55**, 5826 (1997)
130. M. Kamionkowski, J. March-Russell, Phys. Lett. B **282**, 137 (1992)
131. S.M. Barr, D. Seckel, Phys. Rev. D **46**, 539 (1992)
132. R. Holman, S.D.H. Hsu, T.W. Kephart, E.W. Kolb, R. Watkins, L.M. Widrow, Phys. Lett. B **282**, 132 (1992)
133. E.J. Chun, A. Lukas, Phys. Lett. B **297**, 298 (1992)
134. K.S. Babu, I. Gogoladze, K. Wang, Phys. Lett. B **560**, 214 (2003)
135. S.P. Martin, Phys. Rev. D **54**, 2340 (1996)
136. S.P. Martin, Phys. Rev. D **61**, 035004 (2000)
137. S.P. Martin, Phys. Rev. D **62**, 095008 (2000)
138. M.B. Green, J.H. Schwarz, Phys. Lett. B **149**, 117 (1984)
139. L.M. Krauss, F. Wilczek, Phys. Rev. Lett. **62**, 1221 (1989)
140. M. Dine, arXiv:hep-th/9207045
141. R. Kallosh, A.D. Linde, D.A. Linde, L. Susskind, Phys. Rev. D **52**, 912 (1995)
142. C. Vafa, arXiv:hep-th/0509212
143. K. Choi, E.J. Chun, H.D. Kim, Phys. Rev. D **55**, 7010 (1997)
144. L.J. Hall, Y. Nomura, A. Pierce, Phys. Lett. B **538**, 359 (2002)
145. K. Harigaya, M. Ibe, K. Schmitz, T.T. Yanagida, Phys. Rev. D **88**, 075022 (2013)
146. R. Kappl, B. Petersen, S. Raby, M. Ratz, R. Schieren, P.K.S. Vaudrevange, Nucl. Phys. B **847**, 325 (2011)
147. H.P. Nilles, PoS (CORFU2016) 017, in *Proceedings of the Corfu Summer Institute 2016 "School and Workshops on Elementary Particle Physics and Gravity"*, 31 August – 23 September, 2016, Corfu, Greece
148. D. Harlow, H. Ooguri, arXiv:1810.05338 [hep-th]
149. H.M. Lee, S. Raby, M. Ratz, G.G. Ross, R. Schieren, K. Schmidt-Hoberg, P.K.S. Vaudrevange, Phys. Lett. B **694**, 491 (2011)
150. K.S. Babu, I. Gogoladze, K. Wang, Nucl. Phys. B **660**, 322 (2003)
151. G.F. Giudice, A. Masiero, Phys. Lett. B **206**, 480 (1988)
152. H. Baer, V. Barger, D. Sengupta, Phys. Lett. B **790**, 58 (2019)
153. K. Choi, E.J. Chun, J.E. Kim, Phys. Lett. B **403**, 209 (1997)
154. H. Murayama, H. Suzuki, T. Yanagida, Phys. Lett. B **291**, 418 (1992)
155. K.J. Bae, H. Baer, H. Serce, Phys. Rev. D **91**, 015003 (2015)
156. K.J. Bae, H. Baer, E.J. Chun, Phys. Rev. D **89**, 031701 (2014)
157. K.J. Bae, H. Baer, E.J. Chun, JCAP **1312**, 028 (2013)
158. K.J. Bae, H. Baer, A. Lessa, H. Serce, JCAP **1410**, 082 (2014)
159. M.Y. Khlopov, A.D. Linde, Phys. Lett. B **138**, 265 (1984)
160. M. Kawasaki, K. Kohri, T. Moroi, A. Yotsuyanagi, Phys. Rev. D **78**, 065011 (2008)
161. F. Gabbiani, E. Gabrielli, A. Masiero, L. Silvestrini, Nucl. Phys. B **477**, 321 (1996)
162. M. Dine, A. Kagan, S. Samuel, Phys. Lett. B **243**, 250 (1990)
163. S.A.R. Ellis, G.L. Kane, B. Zheng, JHEP **1507**, 081 (2015)
164. O. Lebedev, H.P. Nilles, S. Raby, S. Ramos-Sanchez, M. Ratz, P.K.S. Vaudrevange, A. Wingerter, Phys. Lett. B **645**, 88 (2007)

165. O. Lebedev, H.P. Nilles, S. Ramos-Sanchez, M. Ratz, P.K.S. Vaudrevange, Phys. Lett. B **668**, 331 (2008)
166. S. Ashok, M.R. Douglas, JHEP **0401**, 060 (2004)
167. L. Susskind, in *From Fields to Strings: Circumnavigating Theoretical Physics*, edited by M. Shifman et al. (2005), Vol. 3, pp. 1745–1749
168. F. Denef, M.R. Douglas, JHEP **0405**, 072 (2004)
169. N. Arkani-Hamed, S. Dimopoulos, S. Kachru, arXiv:hep-th/0501082
170. G.F. Giudice, R. Rattazzi, Nucl. Phys. B **757**, 19 (2006)
171. M. Tanabashi et al. [Particle Data Group], Phys. Rev. D **98**, 030001 (2018)
172. H. Bahl, T. Hahn, S. Heinemeyer, W. Hollik, S. Paßehr, H. Rzehak, G. Weiglein, arXiv:1811.09073 [hep-ph]
173. J. Pardo Vega, G. Villadoro, JHEP **1507**, 159 (2015)
174. M. Aaboud et al. [ATLAS Collaboration], Phys. Rev. D **97**, 112001 (2018)
175. A.M. Sirunyan et al. [CMS Collaboration], JHEP **1710**, 019 (2017)
176. The ATLAS collaboration, Search for direct top squark pair production in the 3-body decay mode with a final state containing one lepton, jets, and missing transverse momentum in $\sqrt{s} = 13$ TeV pp collision data with the ATLAS detector, in *Atlas conference, Genêve, mai 2019*, edited by ATLAS Collaboration (CERN, 2019) [ATLAS-CONF-2019-017]
177. H. Baer, V. Barger, D. Sengupta, X. Tata, Eur. Phys. J. C **78**, 838 (2018)
178. H. Baer, V. Barger, S. Salam, H. Serce, K. Sinha, JHEP **1904**, 043 (2019)
179. H. Baer, V. Barger, D. Sengupta, H. Serce, K. Sinha, R.W. Deal, Eur. Phys. J. C **79**, 897 (2019)
180. F. Wilczek, in *Universe or Multiverse*, edited by B. Carr (Cambridge University Press, 2007) pp. 151–162
181. See also F. Wilczek, Class. Quant. Grav. **30**, 193001 (2013)
182. M. Tegmark, A. Aguirre, M. Rees, F. Wilczek, Phys. Rev. D **73**, 023505 (2006)
183. H. Baer, V. Barger, D. Sengupta, arXiv:1705.01798 [hep-ph]
184. M.R. Douglas, C. R. Physique **5**, 965 (2004)
185. H.P. Nilles, P.K.S. Vaudrevange, Mod. Phys. Lett. A **30**, 1530008 (2015)
186. W. Buchmuller, K. Hamaguchi, O. Lebedev, M. Ratz, arXiv:hep-ph/0512326
187. M. Ratz, Soryushiron Kenkyu Electr. **116**, A56 (2008)
188. H.P. Nilles, S. Ramos-Sanchez, P.K.S. Vaudrevange, AIP Conf. Proc. **1200**, 226 (2010)
189. H.P. Nilles, Phys. Lett. B **115**, 193 (1982)
190. H.P. Nilles, Nucl. Phys. B **217**, 366 (1983)
191. S. Ferrara, L. Girardello, H.P. Nilles, Phys. Lett. B **125**, 457 (1983)
192. For a review, see H.P. Nilles, arXiv:hep-th/0402022
193. T. Kobayashi, S. Raby, R.J. Zhang, Nucl. Phys. B **704**, 3 (2005)
194. W. Buchmuller, K. Hamaguchi, O. Lebedev, M. Ratz, Phys. Rev. Lett. **96**, 121602 (2006)
195. W. Buchmuller, K. Hamaguchi, O. Lebedev, M. Ratz, Nucl. Phys. B **785**, 149 (2007)
196. W. Buchmuller, K. Hamaguchi, O. Lebedev, S. Ramos-Sanchez, M. Ratz, Phys. Rev. Lett. **99**, 021601 (2007)
197. H.P. Nilles, Adv. High Energy Phys. **2015**, 412487 (2015)
198. S. Krippendorf, H.P. Nilles, M. Ratz, M.W. Winkler, Phys. Lett. B **712**, 87 (2012)
199. M. Badziak, S. Krippendorf, H.P. Nilles, M.W. Winkler, JHEP **1303**, 094 (2013)
200. H. Baer, V. Barger, M. Savoy, H. Serce, X. Tata, JHEP **1706**, 101 (2017)
201. S. Kachru, R. Kallosh, A.D. Linde, S.P. Trivedi, Phys. Rev. D **68**, 046005 (2003)
202. G. Obied, H. Ooguri, L. Spodyneiko, C. Vafa, arXiv:1806.08362 [hep-th]
203. A. Arvanitaki, N. Craig, S. Dimopoulos, G. Villadoro, JHEP **1302**, 126 (2013)
204. V. Balasubramanian, P. Berglund, J.P. Conlon, F. Quevedo, JHEP **0503**, 007 (2005)
205. K. Choi, H.P. Nilles, C.S. Shin, M. Trapletti, JHEP **1102**, 047 (2011)
206. L. Aparicio, F. Quevedo, R. Valandro, JHEP **1603**, 036 (2016)
207. B.S. Acharya, K. Bobkov, G. Kane, P. Kumar, D. Vaman, Phys. Rev. Lett. **97**, 191601 (2006)

208. B.S. Acharya, K. Bobkov, G.L. Kane, P. Kumar, J. Shao, Phys. Rev. D **76**, 126010 (2007)
209. B.S. Acharya, K. Bobkov, G.L. Kane, J. Shao, P. Kumar, Phys. Rev. D **78**, 065038 (2008)
210. B.S. Acharya, G. Kane, P. Kumar, Int. J. Mod. Phys. A **27**, 1230012 (2012)
211. P. Kumar, Adv. Ser. Direct. High Energy Phys. **22**, 277 (2015)
212. G. Kane, K. Sinha, S. Watson, Int. J. Mod. Phys. D **24**, 1530022 (2015)
213. B.S. Acharya, G. Kane, S. Watson, P. Kumar, Phys. Rev. D **80**, 083529 (2009)
214. B.S. Acharya, G. Kane, E. Kuflik, R. Lu, JHEP **1105**, 033 (2011)
215. H. Baer, J.R. Ellis, G.B. Gelmini, D.V. Nanopoulos, X. Tata, Phys. Lett. B **161**, 175 (1985)
216. G. Gamberini, Z. Phys. C **30**, 605 (1986)
217. H. Baer, V.D. Barger, D. Karatas, X. Tata, Phys. Rev. D **36**, 96 (1987)
218. H. Baer, R.M. Barnett, M. Drees, J.F. Gunion, H.E. Haber, D.L. Karatas, X.R. Tata, Int. J. Mod. Phys. A **2**, 1131 (1987)
219. R.M. Barnett, J.F. Gunion, H.E. Haber, Phys. Rev. D **37**, 1892 (1988)
220. H. Baer, A. Bartl, D. Karatas, W. Majerotto, X. Tata, Int. J. Mod. Phys. A **4**, 4111 (1989)
221. H. Baer, X. Tata, J. Woodside, Phys. Rev. D **42**, 1568 (1990)
222. H. Baer, X. Tata, J. Woodside, Phys. Rev. D **45**, 142 (1992)
223. A. Bartl, W. Majerotto, B. Mosslacher, N. Oshimo, S. Stippel, Phys. Rev. D **43**, 2214 (1991)
224. A. Bartl, W. Majerotto, W. Porod, Z. Phys. C **64**, 499 (1994) [Erratum: Z. Phys. C **68**, 518 (1995)]
225. H. Baer, C.h. Chen, M. Drees, F. Paige, X. Tata, Phys. Rev. D **58**, 075008 (1998)
226. S.A.R. Ellis, G.L. Kane, B. Zheng, JHEP **1507**, 081 (2015)
227. G. Kane, P. Kumar, R. Lu, B. Zheng, Phys. Rev. D **85**, 075026 (2012)
228. H. Baer, V. Barger, J.S. Gainer, H. Serce, X. Tata, Phys. Rev. D **96**, 115008 (2017)
229. H. Baer, V. Barger, N. Nagata, M. Savoy, Phys. Rev. D **95**, 055012 (2017)
230. H. Baer, V. Barger, P. Huang, D. Mickelson, A. Mustafayev, W. Sreethawong, X. Tata, Phys. Rev. Lett. **110**, 151801 (2013)
231. H. Baer, V. Barger, P. Huang, D. Mickelson, A. Mustafayev, W. Sreethawong, X. Tata, JHEP **1312**, 013 (2013) [Erratum: JHEP **1506**, 053 (2015)]
232. H. Baer, V. Barger, J.S. Gainer, M. Savoy, D. Sengupta, X. Tata, Phys. Rev. D **97**, 035012 (2018)
233. H. Baer, A. Mustafayev, X. Tata, Phys. Rev. D **89**, 055007 (2014)
234. T. Han, S. Mukhopadhyay, X. Wang, Phys. Rev. D **98**, 035026 (2018)
235. Z. Han, G.D. Kribs, A. Martin, A. Menon, Phys. Rev. D **89**, 075007 (2014)
236. H. Baer, A. Mustafayev, X. Tata, Phys. Rev. D **90**, 115007 (2014)
237. CMS Collaboration, Search for new physics in events with two low momentum opposite-sign leptons and missing transverse energy at $\sqrt{s}$=13 TeV, in *CMS Physics Analysis Summaries*, Geneve, edited by CMS Collaboration (CERN, 2017) [CMS-PAS-SUS-16-048]
238. M. Aaboud et al. [ATLAS Collaboration], Phys. Rev. D **97**, 052010 (2018)
239. G. Aad et al. [ATLAS Collaboration], arXiv:1911.12606 [hep-ex]
240. The ATLAS collaboration, ATLAS sensitivity to winos and higgsinos with a highly compressed mass spectrum at the HL-LHC, in *Atlas note, Geneve, 2018*, edited by Atlas collaboration (CERN, 2018) [ATL-PHYS-PUB-2018-031]
241. X. Cid Vidal et al., CERN Yellow Rep. Monogr. **7**, 585 (2019)
242. H. Baer, V. Barger, H. Serce, K. Sinha, JHEP **1803**, 002 (2018)
243. K.J. Bae, H. Baer, N. Nagata, H. Serce, Phys. Rev. D **92**, 035006 (2015)
244. K. Fujii et al., arXiv:1702.05333 [hep-ph]
245. H. Baer, V. Barger, D. Mickelson, A. Mustafayev, X. Tata, JHEP **1406**, 172 (2014)
246. H. Baer, M. Berggren, K. Fujii, J. List, S.L. Lehtinen, T. Tanabe, J. Yan, arXiv:1912.06643 [hep-ex]
247. H. Baer, V. Barger, H. Serce, Phys. Rev. Res. **1**, 033022 (2019)

248. C. Han, M. López-Ibáñez, A. Melis, Ó. Vives, L. Wu, J.M. Yang, arXiv:2003.06187 [hep-ph]
249. M. Davier, A. Hoecker, B. Malaescu, Z. Zhang, Eur. Phys. J. C **80**, 241 (2020)
250. S. Borsanyi, Z. Fodor, J. Guenther, C. Hoelbling, S. Katz, L. Lellouch, T. Lippert, K. Miura, L. Parato, K. Szabo, F. Stokes, B. Toth, C. Torok, L. Varnhorst, arXiv:2002.12347 [hep-lat]
251. H. Baer, A. Lessa, S. Rajagopalan, W. Sreethawong, JCAP **1106**, 031 (2011)
252. H. Baer, A. Lessa, W. Sreethawong, JCAP **1201**, 036 (2012)
253. K.J. Bae, H. Baer, E.J. Chun, JCAP **1312**, 028 (2013)
254. K.J. Bae, H. Baer, A. Lessa, H. Serce, JCAP **1410**, 082 (2014)
255. K.J. Bae, H. Baer, H. Serce, JCAP **1706**, 024 (2017)
256. M. Carena, M. Quiros, C.E.M. Wagner, Nucl. Phys. B **524**, 3 (1998); [for an update, see M. Carena, G. Nardini, M. Quiros, C.E.M. Wagner, Nucl. Phys. B **812**, 243 (2009)]
257. M. Fukugita, T. Yanagida, Phys. Lett. B **174**, 45 (1986)
258. M.A. Luty, Phys. Rev. D **45**, 455 (1992)
259. B.A. Campbell, S. Davidson, K.A. Olive, Phys. Lett. B **303**, 63 (1993)
260. W. Buchmuller, P. Di Bari, M. Plumacher, Nucl. Phys. B **643**, 367 (2002) [Erratum: Nucl. Phys. B **793**, 362 (2008)]
261. W. Buchmuller, P. Di Bari, M. Plumacher, Phys. Lett. B **547**, 128 (2002)
262. P. Di Bari, AIP Conf. Proc. **655**, 208 (2003)
263. W. Buchmuller, R.D. Peccei, T. Yanagida, Ann. Rev. Nucl. Part. Sci. **55**, 311 (2005)
264. S. Davidson, E. Nardi, Y. Nir, Phys. Rep. **466**, 105 (2008)
265. S. Blanchet, P. Di Bari, New J. Phys. **14**, 125012 (2012)
266. K. Kumekawa, T. Moroi, T. Yanagida, Prog. Theor. Phys. **92**, 437 (1994)
267. G. Lazarides, Springer Tracts Mod. Phys. **163**, 227 (2000)
268. G.F. Giudice, M. Peloso, A. Riotto, I. Tkachev, JHEP **9908**, 014 (1999)
269. T. Asaka, K. Hamaguchi, M. Kawasaki, T. Yanagida, Phys. Lett. B **464**, 12 (1999)
270. T. Asaka, K. Hamaguchi, M. Kawasaki, T. Yanagida, Phys. Rev. D **61**, 083512 (2000)
271. M. Kawasaki, M. Yamaguchi, T. Yanagida, Phys. Rev. D **63**, 103514 (2001)
272. K. Hamaguchi, H. Murayama, T. Yanagida, Phys. Rev. D **65**, 043512 (2002)
273. M. Dine, L. Randall, S.D. Thomas, Phys. Rev. Lett. **75**, 398 (1995)
274. M. Dine, L. Randall, S.D. Thomas, Nucl. Phys. B **458**, 291 (1996)
275. I. Affleck, M. Dine, Nucl. Phys. B **249**, 361 (1985)
276. K.J. Bae, H. Baer, H. Serce, Y.F. Zhang, JCAP **1601**, 012 (2016)
277. K.J. Bae, H. Baer, K. Hamaguchi, K. Nakayama, JHEP **1702**, 017 (2017)
278. Y. Cui, Mod. Phys. Lett. A **30**, 1530028 (2015)